

OPTIMAL SIZING, MODELING, AND DESIGN OF A  
SUPERVISORY CONTROLLER OF A STAND-ALONE  
HYBRID ENERGY SYSTEM

MOHAMED EL BADAWE



**OPTIMAL SIZING, MODELING, AND DESIGN OF A SUPERVISORY  
CONTROLLER OF A STAND-ALONE HYBRID ENERGY SYSTEM**

By

© Mohamed El Badawe

A thesis submitted to the School of  
Graduate Studies in partial fulfillment of the requirements for the degree of  
Master of Engineering

Faculty of Engineering & Applied Science  
Memorial University of Newfoundland

**September 2012**

St. John's, Newfoundland, Canada

## ABSTRACT

Microwave repeaters are one of the main energy consumers in the telecommunication industry. These repeaters are powered using diesel generators and batteries, particularly when they are located in remote areas. Diesel generators require a higher maintenance cost and for remote sites this cost will be more due to inaccessibility and spare transportation to the added to its operating cost. This thesis researches optimal sizing and compares a non-renewable energy system (existing system) and a renewable energy system (proposed system) for a remotely located telecommunication site in Mulligan, Labrador in Canada. The current system is operated using a diesel generator and batteries and the proposed system is expected to integrate a hybrid wind and solar energy system with the existing diesel generator and batteries. Hybrid Optimization Model for Electric Renewable (HOMER) software is used to obtain the most feasible configuration of a hybrid renewable energy system. Secondly, the proposed hybrid system is modeled in Matlab/Simulink and results are presented to demonstrate the system's performance. Finally, a real time supervisory controller has been designed and implemented for a small scale hybrid power system at Memorial University of Newfoundland. The overall reliability is guaranteed since there are two backup sources; battery bank and diesel generator. The results show the hybrid renewable energy system is cost effective. The proposed system significantly reduces the running time of the diesel generator and this helps to reduce the emission level. Moreover, it is expected that the proposed system will help the BellAliant Company to provide uninterrupted power for their sites in remote areas of Labrador.



## ACKNOWLEDGEMENTS

Firstly the author would like to gratefully remember the Almighty for being accorded all the encouragement, patience and optimism throughout the research.

This work has been carried out at the Faculty of Engineering and Applied Science at Memorial University of Newfoundland, Canada. It has been funded by the Ministry of Education and Scientific Research of Libya. The author would like to thank his parents and sibling for support during the study period.

The author would like to express his thanks to his thesis supervisors; Dr. Tariq Iqbal and Dr. George Mann for their supervision, advice, and encouragement throughout the period of the work. Thanks also go to Mr. Stephen Smith who works with Bell-Aliant for providing the site load data, location, and configuration information, and to Greg O'Leary, Glenn St. Croix, and Craig Mitchell for their kind help.

Also, the author would like to thank all the staff members of the Canadian Bureau for International Education (CBIE), especially the academic manager Ms. Diane Cyr. Furthermore, the administrative cooperation from Moya Croker is highly acknowledged.



## Table of Contents

Abstract	ii
Acknowledgments	iii
Table of Contents	iv
List of Tables	ix
List of Figures	x
List of Symbols	xv
List of Abbreviations	xiv
List of Appendices	xiv
<b>Chapter 1 Introduction and Literature Review .....</b>	<b>1</b>
1.1 Introduction	1
1.2 Background	1
1.3 Global Renewable Energy Development	3
1.4 Motivation	7
1.5 Thesis Objectives	8
1.6 Literature Review	9
1.6.1 Renewable Energy in Telecommunication	9
1.6.2 Optimization and Modeling of Hybrid Renewable Energy Systems	12

1.6.3 Control Methods in Renewable Energy Systems	16
1.6.4 Supervisory Control in Renewable Energy Systems	19
1.7 Thesis Layout	22
<b>Chapter 2 Sizing and Analysis of a Hybrid Power System</b> .....	<b>23</b>
2.1 Introduction	23
2.2 Renewable Energy Information Location	24
2.2.1 Solar energy resource	24
2.2.2 Wind energy resource	26
2.3 System Unit Sizing	27
2.3.1 Electrical load	27
2.3.2 Photovoltaic array	29
2.3.3 Wind turbine	30
2.3.4 Diesel generator	32
2.3.5 Battery bank	33
2.3.6 Power converter	34
2.4 System Optimizations	34
2.4.1 The existing system	34
2.4.2 The proposed system	35
2.5 Optimization and Comparison Results	36

2.5.1 The existing system	36
2.5.1.1 Electrical production	37
2.5.1.2 Emissions	38
2.5.2 The proposed system	38
2.5.2.1 Electrical production	39
2.5.2.2 Emissions	41
2.6 Summary	42
<b>Chapter 3 Modeling of Hybrid Power System</b> .....	<b>44</b>
3.1 Primary Energy Sources	44
3.2 Wind Energy System	45
3.2.1 Energy in wind	45
3.2.2 Tip speed ratio	46
3.2.3 Wind turbine output power vs. wind speed	46
3.2.4 Wind energy conversion system	47
3.2.5 Types of wind turbines	49
3.2.6 Modeling and simulation of Beregy wind turbine	50
3.3 Solar Energy System	53
3.3.1 The fundamentals of PV	53
3.3.2 Photovoltaic modeling	54

3.3.3 Photovoltaic module and array	56
3.3.4 Photovoltaic model in Matlab/Simulink	57
3.3.5 Maximum power point tracking	59
3.4 Diesel Generator	61
3.5 Energy Storage	62
3.6 Summary	64
<b>Chapter 4 Experimental Testing of Proposed Supervisory Controller .....</b>	<b>65</b>
4.1 Introduction	65
4.2 Experimental Setup	65
4.3 Wind Turbine	68
4.4 Photovoltaic Panel	70
4.5 DC Current Transducer (CR5210)	71
4.6 Electromechanical Relay	73
4.7 Relay Driver circuits	74
4.8 Microcontroller	76
4.9 Supervisory Controller	78
4.10 Summary	81
<b>Chapter 5 Results and Discussion .....</b>	<b>82</b>
5.1 Introduction	82

5.2 Modeling Results	82
5.3 Experiment Results	87
5.3.1 Case study 1	87
5.3.1.1 Case study 1 in first 7 minutes	87
5.3.1.2 Case study 1 after 30 minutes	91
5.3.1.3 Case study 1 after 50 minutes	93
5.3.2 Case study 2	94
5.3.3 Case study 3	96
5.4 Experiment Results with Battery Connected and Disconnected	97
5.5 Experiment Results when only Wind Turbine is Connected	99
5.6 Summary	100
<b>Chapter 6 Conclusion and Future Work.....</b>	<b>101</b>
6.1 Conclusion	101
6.2 Research Contribution	103
6.3 Future Work	104
Publications.....	106
Bibliography.....	107
Appendices.....	116

## List of Tables

Table 2-1: Clearness index and average monthly irradiation for a year .....	25
Table 2-2: Monthly average wind speed for a year at 10m height(38).....	26
Table 2-3: Consumption Data .....	33
Table 2-4: Optimized result for the non-renewable energy system .....	37
Table 2-5: Emission values in the existing system estimated by from HOMER tool .....	38
Table 2-6: Optimized result for the renewable energy system .....	39
Table 2-7: Energy production for proposed system from HOMER software.....	39
Table 2-8: Excess energy for proposed system from HOMER software.....	41
Table 2-9: Emission values in the proposed system estimated by HOMER tool .....	42
Table 3-1: Beregy Excel 7.5 wind turbine specifications .....	51
Table 3-2: The PV model parameters .....	58
Table 4-1: Air-X wind turbine specifications .....	69
Table 4-2: Wind speed measurements .....	70
Table 4-3: Current transducer specifications .....	72
Table 4-4: PIC18F4520 specifications.....	77
Table 5-1: Experiment results in first 7 minutes.....	88
Table 5-2: Experiment results after 30 minutes.....	92
Table 5-3: Experiment results after 50 minutes.....	93
Table 5-4: Experiment results when there is no wind.....	94
Table 5-5: experiment results on a cloudy day .....	96
Table 5-6: Experiment results when only the wind turbine is the connected .....	99

## List of Figures

Figure 1.1: World energy consumption, 1990-2035 (quadrillion Btu).....	2
Figure 1.2: Global energy production in 2009.....	4
Figure 1.3: Global energy production in 2010.....	4
Figure 1.4: Renewable energy capacities in developing countries, Europe, top five countries, and in the world.....	5
Figure 1.5: Global installed power generation capacity by energy source.....	6
Figure 1.6: Global installed power generation capacity by renewable source.....	6
Figure 2.1: Monthly solar radiation produced by HOMER.....	25
Figure 2.2: The average monthly wind speed for a year.....	27
Figure 2.3: Monthly Load profile of Mulligan site for a year.....	28
Figure 2.4: Load pattern of a microwave repeater.....	28
Figure 2.5: Daily load profile based on the load data.....	29
Figure 2.6: The cost curve of solar panel.....	29
Figure 2.7: Wind turbine power curve.....	31
Figure 2.8: The cost curve of wind turbine.....	31
Figure 2.9: Shear exponent vs $Z_0$ .....	31
Figure 2.10: The cost curve of diesel generator.....	32
Figure 2.11: Efficiency Curve.....	32
Figure 2.12: The cost curve of battery.....	33
Figure 2.13: The cost curve of converter.....	34
Figure 2.14: Existing power system at Mulligan.....	35

Figure 2.15: Proposed hybrid power system for Mulligan .....	36
Figure 2.16: Monthly average electric production for non-renewable energy system .....	37
Figure 2.17: Monthly average electric production for renewable energy system.....	39
Figure 2.18: Yearly wind turbine output power spectrum from HOMER simulation.....	40
Figure 2.19: Yearly PV output power spectrum from HOMER simulation .....	40
Figure 2.20: Yearly diesel generator output power spectrum from HOMER simulation..	41
Figure 3.1: A photograph of Bell-Aliant’s telecommunication site at Mulligan, Labrador .....	44
Figure 3.2: A typical wind turbine power curve .....	47
Figure 3.3: Schematic diagram of wind energy conversion system .....	48
Figure 3.4: Upwind and downwind type wind turbines.....	49
Figure 3.5: System block diagram of WECS.....	50
Figure 3.6: Wind turbine power curve .....	52
Figure 3.7: WECS output power for different wind speeds.....	52
Figure 3.8: The World total PV cells installed capacity .....	53
Figure 3.9: An illustration of p-n junction solar cell .....	54
Figure 3.10: Solar cell model.....	56
Figure 3.11: PV cell, module and array .....	56
Figure 3.12: PV Module STP280-24V .....	57
Figure 3.13: P-V output characteristics with 1000(W/m <sup>2</sup> ) .....	58
Figure 3.14: P-V output characteristics with 800(W/m <sup>2</sup> ).....	59
Figure 3.15: P-V output characteristics with 600(W/m <sup>2</sup> ).....	59

Figure 3.16: P-V output characteristics with MPPT technique .....	60
Figure 3.17: The effect of solar irradiance.....	60
Figure 3.18: Diesel generator model in Matlab/Simulink.....	61
Figure 3.19: Engine and excitation system of diesel generator .....	62
Figure 3.20: Diesel generator power curve.....	62
Figure 3.21: Battery model in Matlab/Simulink .....	63
Figure 4.1: Schematic diagram of the experiment setup.....	67
Figure 4.2: The experimental setup in the lab with various components .....	67
Figure 4.3: Air-X wind turbine in the wind tunnel .....	68
Figure 4.4: Solar panels on the roof.....	71
Figure 4.5: CR5210 current transducers .....	72
Figure 4.6: CR5210 connection diagram .....	73
Figure 4.7: A typical electromechanical relay .....	74
Figure 4.8: Relay driver circuits .....	75
Figure 4.9: Relays and their driver circuits.....	76
Figure 4.10: EasyPic4 used in the experiment.....	78
Figure 4.11: Schematic diagram of the supervisory controller.....	79
Figure 4.12: Supervisory controller flow chart.....	80
Figure 5.1: System configuration of the proposed alternative hybrid energy system.....	83
Figure 5.2: Current, voltage, and power of the system 10m/s to 12m/s wind speed .....	84
Figure 5.3: Current, voltage, and power of the system 12m/s to 14m/s wind speed .....	84

Figure 5.4: Current, voltage, and output power of the system 1000W/m <sup>2</sup> to 800W/m <sup>2</sup> solar irradiance.....	85
Figure 5.5: The system output when the load is increased .....	86
Figure 5.6: The system output when the load is decreased.....	86
Figure 5.7: PV output current in first 7 minutes .....	88
Figure 5.8: Wind current power in first 7 minutes.....	89
Figure 5.9: Battery state of charge in first 7 minutes.....	89
Figure 5.10: Scope display of PV output .....	90
Figure 5.11: Scope display of wind output .....	90
Figure 5.12: Scope display of wind turbine and PV Output .....	91
Figure 5.13: Battery state of charge after 30 minutes.....	92
Figure 5.14: Battery state of charge after 50 minutes.....	93
Figure 5.15: Battery state of charge when there is no wind.....	94
Figure 5.16: Scope wind and PV output when there was no wind 1 .....	95
Figure 5.17: Scope wind and PV output when there was no wind 2 .....	95
Figure 5.18: Battery state of charge.....	96
Figure 5.19: Scope display of wind and PV output on a cloudy day 1 .....	97
Figure 5.20: Scope display of wind and PV output on a cloudy day 2.....	97
Figure 5.21: The load brightness when the renewable systems and battery are connected .....	98
Figure 5.22: The load brightness when only the renewable systems are connected.....	98

Figure 5.23: Scope display of wind and PV output when only the wind turbine is the connected .....	99
---	----

## Glossary

### List of Symbols

$h_1$	Hub height
$h_2$	Reference height
$U_2$	Scaled wind speed
$U_1$	Wind speed data at highest $h_1$
$\alpha$	Shear exponent
$E$	Kinetic Energy
$m$	Mass
$v$	Speed
$A$	Cross Section Area
$\rho$	Air Density
$P_w$	Wind Power
$C_p$	Power Coefficient
$P_m$	Mechanical power
$\lambda$	Tip Speed Ratio
$\beta$	Pitch Angle
$R$	Rotor Blade Radius
$I$	Cell Output Current
$V$	Cell Output Voltage
$I_s$	Saturation Current
$q$	Electronic Charge
$R_s$	Series Resistance

$K$	Boltzmann's Constant
$T_C$	Cell Temperature
$A$	Ideal Factor
$R_{SH}$	Shunt Resistance
$I_{SC}$	Short Circuit Current
$K_t$	Short-Circuit Current Temperature Coefficient
$T_{Ref}$	Room Temperature 25°C
$\Lambda$	Solar Irradiation
$I_{RS}$	Cell's Reverse Saturation Current
$E_G$	Band Gap for Silicon
$E_{Batt}$	Nonlinear Voltage
$E_0$	Constant Voltage
Exp(s)	Exponential Zone Dynamics
K	Polarization Constant or Polarization Resistance
$i^*$	Low Frequency Current Dynamics
$i$	Battery Current
$it$	Extracted Capacity
Q	Maximum Battery Capacity
$\Lambda$	Exponential Voltage
B	Exponential Capacity
$V_2$	Wind Speed at location of Wind Turbine in The Tunnel

$V_1$	Wind Speed at the Middle of the Tunnel
$A_1$	Area at the Middle of the Tunnel
$A_2$	Area of the Wind Turbine's location in The Tunnel

### **List of Abbreviations**

AC	Alternative Current
ADC	Analog to Digital Converter
Btu	British thermal units
CO <sub>2</sub>	Carbon dioxide
DC	Direct Current
EMF	Electromagnetic Force
FC	Fuel Cell
FPGA	Field Programmable Gate Array
HOMER	Hybrid Optimization Model for Electric Renewable
IMP	Optimum Operating Current
ISC	Short-Circuit Current
LED	Light emitting diodes
MPPT	Maximum Power Point Tracker
NASA	National Aeronautics and Space Administration
NREL	National Renewable Energy Laboratory
OECD	Organization for Economic Cooperation and Development
O&M	Operation & Maintains

PBC	Passivity-Based Control
PCH	Port-Controlled Hamiltonian
PLC	Programmable Logic Controller
PMG	Permanent magnet generator
PV	Photovoltaic
PWM	Pulse Width Modulation
SCADA	Supervisory control and data acquisition
SOX	Sulfur oxides
TNPC	Total Net Present Cost
TSR	Tip Speed Ratio
VMP	Optimum Operating Voltage
VOC	Open-Circuit Voltage
WECS	Wind Energy Conversion Systems
WTG	Wind turbine generators

## **List of Appendices**

Appendix A	Simulation diagram of the hybrid energy system
Appendix B	mikroBasic program for the PIC18F4520 microcontroller

## **Chapter 1 Introduction and Literature Review**

### **1.1 Introduction**

The ability of a system to cause exterior impacts such as a force moving across an area is called energy, and can be categorized as mechanical energy, electrical energy, kinetic energy, nuclear energy, chemical energy etc. [1,2]. While energy is essential to everyone's life, electrical energy is one of the most important energy forms that people need daily. In this chapter, an overview of the world's energy demand, renewable energy systems, controlling methods, and a supervisory controller for hybrid power systems is explained. The scope of the research is also defined.

### **1.2 Background**

The world's energy consumption is expected to grow by about 53% in the next 23 years. Figure 1.1 shows the projected growth of energy demand from 1990 till 2035. The energy demand may rise from 505 quadrillion British thermal units (Btu) in 2008 to 770 quadrillion Btu in 2035. Moreover, future energy consumption will be driven by the demand of non-Organization for Economic Cooperation and Development (OECD) which is an international economic organization that stimulate economic progress and world trade. In 2008, the energy use in non-OECD nations was 7 percent greater than that in OECD nations, while in 2035 it will be 67 percent more[3].

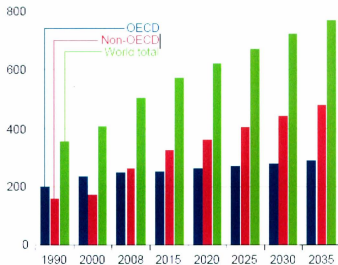


**Figure 1.1: World energy consumption, 1990-2035 (quadrillion Btu)(3)**

The world energy demand rose rapidly after the Second World War. The oil crises started in the beginning of the 1970s and the industrial countries added nuclear power to conventional energy sources. Since then the world has been experiencing higher prices of conventional fossil fuel as well as negative impacts on the environment [1,4]. In the last few years some oil producing countries reported depletion in their usual fossil fuel production, which will lead to increasing oil prices. Moreover, industrialized countries reported that the world has already experienced many environmental problems such as toxic gases produced from fossil fuel which cause air pollution and global warming. Toxic gases include sulfur oxides (SOx), nitrogen oxides (NOx), and the most dangerous one, carbon dioxide (CO<sub>2</sub>), because it is the main gas for the greenhouse effect and it is

not easy to control. However, power energy consumption around the world has been increasing as shown in figure 1.1, while the production of fossil fuel has been decreasing. Renewables 2011 Global Status Report [5] states that approximately 1.5 billion people do not have or have a lack of access to electricity, and most of these people live in rural and remote areas. Moreover, connecting rural areas to electric grids is not easy and is very costly. These factors have led engineers to find sustainable and environmentally friendly solutions such as renewable energy.

The term “renewable energy” refers to electricity supplied by renewable energy sources such as wind, sunlight, geothermal sources, tides, hydropower, and various forms of biomass. A hybrid energy system is a system that contains two or more renewable/non-renewable energy resources. Wind and solar energy are the most rapidly developing areas in renewable energy. Renewable energies offer the promise of clean and abundant energy without negative impacts on the environment and oil prices. Most importantly, renewable energy is very important to generate power for remote communities and remote service such as telecommunication repeaters [6 and 7].

### **1.3 Global Renewable Energy Development**

In recent years, renewable energy is growing in use very quickly, due to increasing oil prices and awareness of greenhouse effects. According to [5], in 2009, 16% of global energy consumption was supplied by renewable energy, 2.8% was supplied by nuclear power, and the rest was supplied by fossil fuel. Figure 1.2 shows global energy production in 2009, while Figure 1.3 shows global energy production in 2010. Almost

20% of global energy consumption was supplied by renewable energy in 2010, which is a 4% increase from 2009.

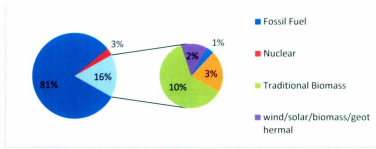


Figure 1.2: Global energy production in 2009(5)

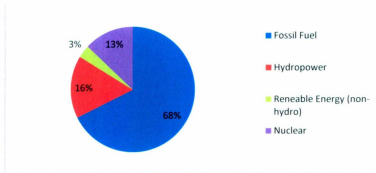
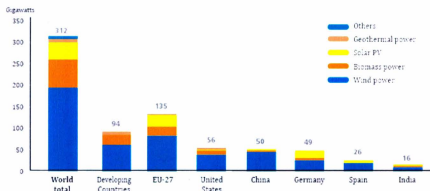


Figure 1.3: Global energy production in 2010(5)

The 2010 renewable energy capacities in developing countries, Europe, top five countries: United States, China, Germany, Spain, and India, and in the world overall are shown in Figure 1.4. It shows renewable energy supplied over 10.3% of total domestic electricity at the end of 2010. China was leading the world in the installation of wind turbines with a capacity of 29 GW, while Germany was leading the installation of solar panels.



**Figure 1.4: Renewable energy capacities in developing countries, Europe, top five countries, and in the world(5)**

Based on [3] global hydroelectric and other renewable energy capacity will rise 2.7% per year by 2035. Figure 1.5 shows the global installed power generation capacity by energy source, while Figure 1.6 shows the global installed power generation capacity by renewable source. The study shows that PV is expected to increase 8.3% per year, plus 5.7% for wind, 3.7% for geothermal and 2.0% for hydropower from 2008 to 2035.

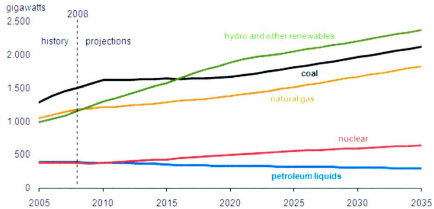


Figure 1.5: Global installed power generation capacity by energy source(3)

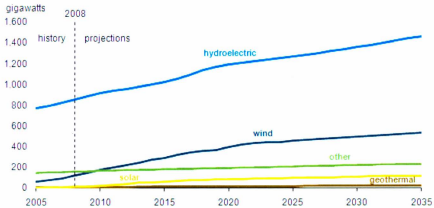


Figure 1.6: Global installed power generation capacity by renewable source(3)

Renewable energy sources have become attractive for power generation in recent years. Therefore, many research projects in renewable energy have been carried out in the last decades. Before starting the project a literature review is done in several sections which are optimization, sizing, dynamic modeling, and controlling of a hybrid renewable energy

system. In addition, some of the research work has been done for both off grid and grid applications. The section below highlights some of this research work.

#### **1.4 Motivation**

Increasing energy consumption and higher prices of conventional fuel since the oil crisis in the 1970s have generated interest in renewable energy. Further, conventional fuel has impacts on the environment. It is also reported that fossil fuel resources have been depleting in major oil producing countries and this will eventually lead to a greater scarcity of energy resources in the world. The environmental issue is one of the major concerns, particularly the emission of carbon dioxide. Moreover, many communities around the world still have no access either to electricity or to communication services. All the above reasons have led engineers and environmentalists to find a sustainable and friendly environmental solution, and they came up with renewable energy.

Communication technology is one of the fastest growing technologies these days. The telecommunication companies are continuously challenged to provide uninterrupted services to rural and remote areas where there is no reliable electrical power supply available. Therefore, renewable energy systems are becoming increasingly popular in these industries to provide uninterrupted power to remote areas. Currently in most cases the telecommunication stations use diesel generators connected with backup batteries to provide power. Telecommunication companies are now attempting to provide uninterrupted power using renewable energy resources.

Multi-source alternative energy subsystems with a proper controller have a good potential to provide higher quality and reliable power to customers than the use of only

one renewable energy source, because some renewable energy resources are seasonal sources. A stand-alone hybrid power system is proposed in this research to provide uninterrupted power for a telecommunication site, and a supervisory control unit has been built and tested at Memorial University of Newfoundland.

The main goals of this research are to design a stand-alone hybrid alternative energy system for the Bell-Aliant telecommunication site in Mulligan, Labrador, Canada, compare the current and the proposed system, and design and test a real time supervisory control system for a small hybrid power system. The current telecommunication site facilities use a diesel generator and batteries for power generation and this research proposes to improve the efficiency and operational costs of this system by integrating renewable energy sources using a wind turbine and a Photovoltaic (PV) panel. In this case wind and PV are considered as the main power sources for the system and a diesel generator and a battery bank are also integrated as a backup power supply. The diesel generator is treated as a mechanism to provide long-term power storage and the battery is used as a backup for short-term power storage. Sizing of the system has been done by HOMER and then modeling has been done in MATLAB/SIMULINK. Because there are no wind turbines and PV systems with the same rated power capacity that is used in the proposed system at Memorial University, a real time supervisory control was designed and tested on a smaller system (400W wind turbine and 120W PV arrays).

### **1.5 Thesis Objectives**

The main objectives of this research are:

- Sizing and profitability study for a stand-alone telecommunication site in Labrador, Canada.
- Modeling of the system using Matlab/Simulink.
- Design of a supervisory controller.
- Experimental testing of proposed supervisory controller.

## **1.6 Literature Review**

The following literature survey for the research consists of various papers published in the different conferences and the journals.

### **1.6.1 Renewable Energy in Telecommunication**

Communication technology is one of fastest growing technologies today. Telecommunication companies are continuously challenged to provide uninterrupted services to rural and remote areas where no reliable electrical power supply is available. Therefore, renewable energy systems are becoming increasingly popular in communication industries to provide uninterrupted power to remote areas. Currently, in most cases the telecommunication stations use diesel generators connected with backup batteries to provide power. Telecommunication companies are now attempting to provide uninterrupted power by using renewable energy resources [6]. J.K. Kaldellis in [8], states that there are more than 5000 mobile telecommunication stations in Greece which cover almost 99% of the country, and more than 10% of these mobile telecommunication stations are off the grid. In [8] he optimize size and study the efficiency of using renewable energy sources instead of diesel generators for a mobile telecommunication

station in Rhodes Island, Greece. A photovoltaic technology has been used at this site because Greece is well known for its high solar potential. Photovoltaic solution for this site has shown many advantages, including: no interference with the radio station since there are no moving parts, low maintenance, and less pollution. .

Since the 1970s, France Telecom Company has been researching the potential of renewable energy for powering its remote sites in [9]. The authors give a brief history of France Telecom and recent research developments. In 1975 the company started its first PV system for microwave stations, and during the period between 1976 and 1980, hybrid wind/PV was applied to its communication stations. Moreover, the company has developed the DIMOSL software to size a site's equipment. In [10], the authors discuss and study the energy consumption by radio telecommunication tools in Italy. The study includes different communication companies, such as Vodafone, H3G, Telecom, and Wind that are using different communication technologies in different locations around Italy. The authors go on to show that the application of renewable energy that is used to produce part of the electricity in two of Vodafone's radio telecommunication sites in Italy is reliable. Photovoltaic systems were applied at both sites and it has been found that the energy productivity is dependent on geographical location. As a result of Photovoltaic systems at these sites the emission reduced by about 2 tons of CO<sub>2</sub> annually. The objective of paper [11] was to design and optimize a hybrid power system combination of: photovoltaic, battery, and liquefied petroleum gas in remote mobile telecommunication sites. The authors in [11] also proved that the hybrid system of two redundant sources, one of them renewable, can guarantee the load demand at all times.

This hybrid system was applied in Breunschweig, Germany to produce electricity to remote radio telecommunication equipment and found the hybrid system to reduce total cost by 55% as compared to a purely PV system. The paper [11] also shows two possible approaches to reach power availability needs at the Breunschweig site: increasing the PV size or using additional energy sources. Because the PV cost is high, using additional energy sources is a better solution to meet the demand load at this particular site.

Ericsson Company is one of the leading telecommunication companies around the world; this company has increased its offering of solar power solutions to its telecommunication towers [12]. As of the year 2000, Ericsson has around 50 sites in North Africa using solar powered radio base station solution. The objective of [12] is to decrease electricity consumption for telecommunication sites to bring about a decrease in emissions. Ericsson has increased the energy efficiency of the energy producers by reducing the electricity consumption at its sites. A solar powered site solution is the main target of Ericsson because it is more economical and reliable than a grid connection. Paper [13] describes a proposed hybrid renewable energy system based on wind and photovoltaic, as a microwave repeater is currently using diesel generator and batteries. This site, owned by BellAliant company, is located in the Labrador region of Canada, and delivers telecommunication services to this remote region. A prefeasibility study was performed using HOMER software to determine the plant sizing. The results of this system show that wind and a PV hybrid system along with diesel and batteries will reduce diesel run times by approximately 80%. Much research has been carried out by researchers in India to provide uninterrupted power to remote telecommunication

facilities. Authors of [14] and [15] designed and optimized a stand-alone wind/PV hybrid renewable energy system for mobile base station sites in off grid areas located in central India. Diesel generators are used for both current systems, while the diesel generators will be used as a long term storage system in the proposed system. The meteorological data of wind speed, Solar Insolation, and load pattern are taken for Bhopal, Central India. Then the data were used in HOMER software to optimize the hybrid energy system. The results of both papers have shown that using a hybrid renewable energy system reduces fuel costs by 70% to 80% compared to diesel generators alone, and also reduces the emission of CO<sub>2</sub>. In [14] the results show that the combination of 13% PV, 56% wind, and the rest by generator is needed to fulfill the electrical energy load demand, while in [15] the combination of 30%PV, 50%wind, and 19% by generator are chosen. In [15] the authors have compared three stand-alone photovoltaic systems using different hybrid energy storage technologies which are battery, fuel cell, and battery-fuel cell. These three systems are used to feed a stand-alone telecommunication base station. The system was simulated in HOMER software to obtain the best possible configuration sizing optimization. The study was done with and without Maximum Power Point Tracker (MPPT) in three systems. The simulation results showed that a Photovoltaic-Fuel cell-Battery with MPPT is the most economic solution.

### **1.6.2 Optimization and Modeling of Hybrid Renewable Energy Systems**

The optimization of hybrid renewable energy systems usually based on the cost of the systems. Therefore, system with lowest cost is the optimal sizing system. The paper [16] addresses the problems of the stand-alone power system and suggests some

applications of it. This system was built on the VSB-TUO campus. The hybrid system in this paper contains wind power, a photovoltaic, a battery, a control unit, and a street light. This paper explains the major steps necessary to design off-grid power system (for wind, solar, charge controllers, and batteries).

In [17], the authors propose an AC-link hybrid power system for stand-alone applications. The hybrid system is composed of wind, photovoltaic, fuel cell, electrolyzer, and a battery. In this system the wind and PV are the primary power resources. The fuel cell works with the electrolyzer as backup and long term storage, while the battery is used for short term backup. An overall power management for different scenarios is discussed in this paper as well as the system sizing and configuration. Also, the system component characteristics are discussed. MATLAB/SIMULINK was used to develop the hybrid system.

In [18], the authors find that the stochastic method is the best for solving time consumption and complex problems in a photovoltaic hybrid system. This method was tested on a standalone street lighting system, and the hybrid system used is a combination of photovoltaic cells, a battery, and a fuel cell. The purpose of this hybrid system is to charge the battery during the day by PV and discharge it during the night. However, if the battery reaches the absolute minimum, it will be charged by both PV and the Fuel cell until it reaches the maximum. The stochastic method was applied to design a hybrid system based on the analysis of the cost function, including some parameters that were neglected in other methods, such as the PV tilt angle and start/stop cycles of the fuel cell

and the battery. The results show that the stochastic method is one of the best methods to optimize a hybrid system.

In [19], the authors develop a hybrid power system based on a dynamic evaluation for six months hourly data of wind speed and solar irradiance. Weather data and manufacturer's specifications of wind turbine and PV module were used to calculate the average amount of power produced during each hour. This hybrid system consisted of a wind turbine, a battery, and a photovoltaic panel. The deterministic algorithm was used in this paper to minimize the life cycle cost of the whole system (wind and PV) and to guarantee the power load. The results show that the life cycle cost of the system depends on the cost of each component, load power, and the particular site.

In [20], the authors compare three stand alone wind turbine generators (WTG) systems using different hybrid energy storage technologies, which are battery, fuel cell, and battery-fuel cell. These three systems delivered power to a stand-alone load of 45.6kWh/day with a 2.3 kW peak power demand. The system was simulated in HOMER software to determine the sizing optimization with different sensitivity scenarios. The simulation results suggest that the Wind Turbine Generator-Fuel cell-Battery has the lowest system cost among the three systems.

Different methodologies for optimal sizing and dynamic modeling of hybrid power systems are presented in papers [21-24 and 6]. In [21], the authors propose a hybrid renewable energy system for an off grid application at a remote area in Malaysia. The system is comprised of a wind turbine and photovoltaic array, while a diesel generator and batteries were also used as backup. The average monthly wind speed and solar

irradiation were collected at the site during 2004. 1253kWh/day with a 197 kW peak was the load profile for this site, and was implemented using HOMER software with sensitivity analysis to determine the optimal hybrid renewable energy configuration. The simulation results show that \$997,085 is the lowest Total Net Present Cost (TNPC) for a hybrid power system that can handle the load demand. The aim of the paper [22], is to deal with sizing and modeling a hybrid renewable energy system in St.John's, Newfoundland. The system is a combination of two wind turbines, one solar panel, one micro hydro, a battery, and a convertor, and the system is grid connected. The typical home heat load, hourly wind speed, solar insolation and the flow rate in the Waterford River were used in HOMER software for sizing the hybrid system. Optimized results determine the following annual energy production of the system: 43% hydro, 30% wind turbines, and 7% generated from PV. Moreover, 20% of the total energy is excess energy and will return to the grid. The modeling results obtained using MATLAB/SIMULINK are presented, and a brief discussion of multiple input DC-DC converters is given in this paper. The authors in [23] develop a new approach to sizing optimization of an off grid hybrid renewable energy system, located in Haute-Normandie, France. The purpose of this approach is to minimize the life cycle cost of the system by making use of a deterministic algorithm and also to guarantee the availability of energy for the site. The hybrid energy system consisted of a wind turbine, photovoltaic panels, and battery, which were each modeled mathematically. The deterministic algorithm was implemented, and the obtained results were discussed in this paper. The aim of paper [6] is to optimize and model a hybrid energy system for a microwave repeater located in Mulligan, Labrador,

Canada. The hybrid system was a combination of wind, solar, diesel generation and batteries. Hybrid Optimization Model for Electric Renewable (HOMER) software was used for the sizing, and sensitivity analysis was performed in order to obtain the most feasible configuration of a hybrid renewable energy system. The proposed hybrid system is finally modeled in SIMULINK and results are presented to demonstrate system performance. In [24], the authors present the design of a 100% renewable energy hybrid system for off grid street lights in St. John's, Canada. The proposed system consists of a photovoltaic module, a wind turbine and a battery. The system also uses a lead acid battery and an ON/OFF controller. System dynamic simulation and steady state simulation for a year are presented in the paper. The sizing was determined using the HOMER software tool and the system modeling and control was performed using MATLAB/SIMULINK. The results indicate that a 28W LED street light can be powered by a small 200W wind turbine and a 50W PV module.

### **1.6.3 Control Methods in Renewable Energy Systems**

In paper [25], the authors discuss the improvement of hybrid power system efficiency based on AVR MCU to develop a digital controller. A Double-BUCK circuit is used to build this controller for two reasons: to achieve the coordination control between wind and PV and to track the maximum power point between solar and battery. The paper also presents the hardware circuit of the system, which contains a Mega8 MCU in the control circuit as the main control chip. This chip has three channels of pulse width modulation (PWM). There are three MOSFETs used in the charge circuit. Some energy management strategies are presented in the paper: the coordination between wind and PV based on

Double-BUCK as mentioned above, battery charge management, and the unloading of wind energy.

In [26], the authors prove the purpose of this paper which is the control of the DC voltage and the energy. The authors propose a new kind of controller for street lighting applications using Passivity-Based Control (PBC). A photovoltaic panel and battery are proposed in this system. The paper first presents the system model; after that, the Port-Controlled Hamiltonian PCH form is written to show the system characteristics and to simplify the stability proof. The authors show the results from using passivity theory and simulation. The paper presents the controller without using sensor devices. A bidirectional DC-DC converter is used to hybridize the PV and the battery and to charge the battery. Also the paper shows the state space model of the system. Finally, they presented results for this system which suggest this controller can reduce the setup cost and manage the energy among different sources.

In [27], detailed theoretical and experimental analyses of hybrid street light system are presented. This paper shows that using hybrid system for street lighting will provide uninterrupted power for this site, and it shows the control strategy and the energy management for all devices. The results of the simulation and experimentation are presented. The association of fuel cell FC, solar panel, and batteries are presented for this hybrid system. The controller is used in this model to ensure a desired voltage and to manage energy between all the devices for the charge/discharge phase and the lamp. In [28], the authors have developed a new method to model and control an integrated renewable energy system that consists of a photovoltaic and a wind power system. First

of all, the system was simulated in MATLAB/SIMULINK to analyze the dynamic behavior of this system. Then, the system was developed in a DK5 modeling/ design environment, which is based on Handel-C programming. The new approach is developed for a unique model, by using the Field Programmable Gate Array (FPGA) of a digital controller, for reusability of the model design, and for generation of valuable IP. The developed controller is downloaded in hardware throughout a RC100 board and provides real-time testing. The new controller was implemented in the hardware experiment and gave results similar to Matlab's.

In [29], a microcontroller was used to control the power electricity flow to the load. The authors' objective was to reduce the electricity bill by using a photovoltaic power system to deliver the required load power. A battery storage bank, a sun tracking system, a DC to AC inverter, and a microcontroller were used to build an integrated energy system. The primary power system in this system is photovoltaic panel, but if the load demand accesses the photovoltaic energy, the controller switches to the utility power. Moreover, the microcontroller (PIC 16F84) controls the sun tracker to capture more perpendicular sun rays to maximize the photovoltaic output power. The results show that adding the sun tracker improved the photovoltaic output power by around 20%.

In [30], the authors develop a lighting system, consisting of light emitting diodes (LED), a photovoltaic array, a battery, and an inverter. This system is grid-connected to guarantee the electricity when the weather is cloudy. In other words, the system is connected to the grid to guarantee the electricity if the PV cannot supply the power demand. There is an inverter in this system to change the direct current (DC) to alternative current (AC) using

current hysteresis control. PLC control was used as a switch between the grid and the rest of the system. The results show that the combination of PLC controller and the inverter is a simple and effective method to connect a power grid and a battery to light LED.

#### **1.6.4 Supervisory Control in Renewable Energy Systems**

In papers [31 and 32] hierarchical control is used as a supervisory control in two different hybrid power systems. In [31], the hybrid power system, which is grid connected, consists of a wind turbine, photovoltaic panels, and battery bank. Five modes of operation are implemented in this supervisory control to maximize use of renewable energy and to minimize the grid connection. When wind power is enough to meet the load demand, the photovoltaic and the grid are inactive while the battery recharges. This mode runs until the wind power cannot handle the load demand. In Mode2, when wind power is not enough to meet the load demand, the supervisory control turns on the photovoltaic subsystem, deactivates the grid, and keeps the battery charged. In Mode3, when wind and photovoltaic subsystems are set to operate at their maximum energy, the grid still deactivates while the battery is set to supply the load. In Mode4, when renewable sources cannot handle the load demand, the supervisory control connects the grid, and makes the battery current equal to the maximum discharge current. In Mode5, when the load demand is much higher than the power available from renewable sources, the supervisory control connects the grid, and the battery current is set to zero.

In [32], the hybrid power system consists of a couple of wind turbines, a diesel generator, and a battery. A hierarchical controller in this system combines supervisory control and local control. The reason for using the supervisory control here is to

maximize fuel savings and minimize unmet load. The results of this approach are verified using Supervisory control and data acquisition (SCADA) simulation to prove the method's performance.

In paper [33], a small scale stand-alone hybrid energy system for a telecommunication tower is developed. A combination of a wind turbine and a battery is used with the use of a supervisory controller, which provides high performance power delivery to the load. The system is implemented with dSPACE hardware to demonstrate the performance of a supervisory controller. In [34], the authors developed real time supervisory control and data acquisition (SCADA) for a hybrid energy system. Two wind induction generators, a photovoltaic panel, an AC to DC converter, a DC to AC inverter, and a battery are simulated in this study. A monitor and controller are implemented through the campus network of National Cheng Kung University. A fuzzy controller is implemented in the programmable logic controller (PLC). It is used to control the required value of excitation capacitors of wind induction generators. It is concluded from the simulated and experimental results that the monitor and control system can be implemented in various renewable energy forms, especially those located in remote areas.

Paper [35] presents a supervisory control system for a hybrid renewable energy system that is a combination of a wind subsystem, a photovoltaic subsystem, and a battery bank. Three different modes are implemented in this controller. In mode1, the wind turbine is set to track the load demand while the solar module is inactive and the battery is in recharge, thus becoming a part of the load demand. If the load demands exceed the wind power, the supervisory control switches to mode2. The wind subsystem is working at

maximum generation and the solar module is set to track a power reference, while the battery bank is in recharge in mode2. Once the generation of the hybrid system is exceeded by power demand, the supervisory control switches to mode3. In mode3, when the wind and solar module are set to operate at their maximum generation, the battery bank is acting as power supply. The supervisory control has the main task of switching the system from one mode to another depending on the system conditions.

In [36], detailed theoretical and experimental analyses of a stand-alone hybrid system are presented. The hybrid renewable energy system is comprised of wind and solar subsystems with battery storage. The real time supervisory control presented uses dSPACE hardware. The supervisory control has the same operation modes as [35]; the only difference is that the photovoltaic is the primary source instead of wind.

The above literature reviews have been split into many different sections. Also, most of the control methods have not been implemented for real time systems. Our project work has addressed a comprehensive hybrid renewable energy system, optimization, sizing, and dynamic modeling for an off grid system. Optimization and sizing have done by HOMER software based on the cost of system components and desirable output power. The dynamic modeling of the system has done by MATLAB/SIMULINK and different scenarios have been tested such as; changing in wind speed, solar irradiation, and load. Then, a real time supervisory control has been designed and implemented in the fluid lab at Memorial University of Newfoundland. The supervisory controller designed and implemented for a different hybrid power system.

### **1.7 Thesis Layout**

Six chapters are presented in this thesis. Chapter 1 includes the introduction, discusses the literature review, and explains the thesis motivation. In chapter 2, the author tries to determine the best optimal sizing and pre-feasibility study of the proposed system using HOMER software tools. Also, a comparison between the current and the proposed system for the particular site is done in Chapter 2. In Chapter 3, the author gives an overview of wind turbines, Photovoltaic systems, diesel generators, and batteries. After that, modeling of all components is done separately at first, and then the modeling of the whole system is explained in Chapter 3 as well. In Chapter 4, the author design, build, and test a real time supervisory control for a hybrid power system which consists of wind turbine, photovoltaic arrays, battery, and power supply, used instead of a diesel generator. Wind turbine specifications, photovoltaic array specifications, power electronic circuits, current sensors, and the microcontroller circuit are explained in Chapter 4. In Chapter 5, the simulation and supervisory controller results under different scenarios of the research work are presented and discussed. Chapter 6 concludes the thesis and gives brief vision of future work.

## Chapter 2 Sizing and Analysis of a Hybrid Power System

### 2.1 Introduction

When designing a hybrid energy system, there are many criteria that need to be considered: power demand must meet the budget range, types and sizes of the system components suitable for the specific location. Therefore, evaluating different system configurations to get the lowest total net present cost of the system is necessary. The Hybrid Optimization Model for Electrical Renewable (HOMER) simulation tool [37] is able to evaluate the economics and technical feasibility of any hybrid power system. HOMER was developed by the American National Renewable Energy Laboratory (NREL) in 1993. This simulation tool can be used for both grid-connected and off-grid systems.

Optimal off-grid energy system configurations for powering a telecommunication site in a remote area in Labrador, the Mulligan telecommunication site, Canada is presented in this research. The HOMER software is used to determine the best optimal sizing and pre-feasibility study of the system. Sensitivity analysis is considered when designing the system in order to find the factors with the highest impact on the system's performance. To simulate any hybrid energy system, HOMER needs to be fed the required data. As wind and solar are the renewable energy sources in this research, HOMER needs the weather data at the specific location.

## **2.2 Renewable Energy Information Location**

The most important factor when developing a hybrid energy system is the proposed location. Choosing a place depends on the availability of the renewable energy resources. Some resources such as hydro are available in specific places for most of the time, while others may vary dramatically season-by-season, such as wind and solar. Canada has many renewable energy resources but at this particular place wind and solar energy are abundantly available. Collecting weather data is one of the main tasks for this pre-feasibility study of a proposed renewable energy system.

### **2.2.1 Solar energy resource**

The latitude and longitude of Mulligan village are  $53^{\circ}.86'N$  and  $59^{\circ}.92'W$  respectively in time zone GMT3:30 Newfoundland. The hourly solar radiation data is collected for 2010 from National Aeronautics and Space Administration (NASA) [38]. The average solar irradiation is only  $2.85kWh/m^2-d$  and sensitivity analysis is done with three different values. The clearness index and the average daily radiation for a year are shown in table 2.1, while figure 2.1 shows the solar radiation in a year produced by HOMER.

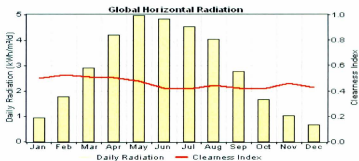


Figure 2.1: Monthly solar radiation produced by HOMER

Table 2-1: Clearness index and average monthly irradiation for a year

Month	Clearness Index	Daily Radiation (kWh/m <sup>2</sup> -d)
January	0.496	0.950
February	0.525	1.760
March	0.509	2.890
April	0.502	4.200
May	0.474	4.980
June	0.421	4.830
July	0.412	4.530
August	0.442	4.040
September	0.418	2.750
October	0.412	1.660
November	0.458	1.020
December	0.427	0.650

### 2.2.2 Wind energy resource

Wind is the second renewable source implemented in the system. Specific wind data for this site is still being collected. Therefore, scaling up the wind speed data from Windatlas approximates the wind speed at Mulligan's telecommunication site. Figure 2.2 shows the average hourly wind speed for a year to be estimated at 6.261m/s, and three values of wind speed are chosen for sensitivity analysis. The monthly average wind speeds are shown in table 2.2.

**Table 2-2: Monthly average wind speed for a year at 10m height(38)**

Month	Wind Speed (m/s)
January	6.910
February	6.500
March	6.665
April	6.256
May	5.847
June	5.970
July	5.520
August	5.561
September	6.011
October	6.338
November	6.788
December	6.788

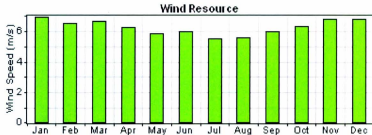


Figure 2.2: The average monthly wind speed for a year

### 2.3 System Unit Sizing

The proposed system primarily employs renewable sources (Wind/PV), which are supported by standby non-renewable sources (diesel generator/Batteries). A converter is included in the system to connect the AC and DC links. The sector details are all the gathered information required to run the HOMER simulation tool including: load profile, solar resource input, wind resource input, diesel generator data, battery data, converter data, as well as components' cost and system constraints.

#### 2.3.1 Electrical load

The Mulligan site daily average DC load is 69A, and the system runs on 48V DC bus. So, the approximate power consumption at this site is 79.5kWh/day [39]. Data Synthesizer is used to extract the load data, and then that data is used in HOMER. It is known that telecommunication companies operate continuously throughout the year; the hourly load is a virtual constant. Figure 2.3 shows a typical load profile produced by HOMER for the telecommunication site. The detailed hourly variations of load data throughout the year are shown in figure 2.4. It is clear that the variation is very small in

some months- never more than  $\pm 0.1\text{kW}$ . Most of the time, the variations in load are mainly due to the heaters and air conditioners usage within the system. The daily load variation is shown in figure 2.5.

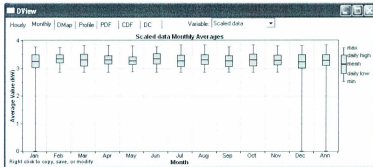


Figure 2.3: Monthly Load profile of Mulligan site for a year

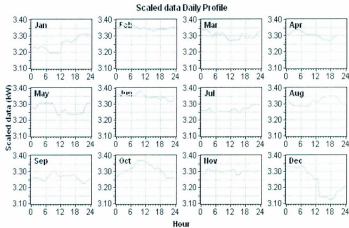


Figure 2.4: Load pattern of a microwave repeater

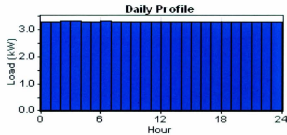


Figure 2.5: Daily load profile based on the load data

### 2.3.2 Photovoltaic array

STP280-24Vd solar modules are used in this system, and each module panel provides 280W with 24V. Therefore, two PV modules are connected in series to meet the bus voltage of 48V. A total rated capacity of 5.6kW PV is used in this system. Modules are connected in 10 strings. Each string has two modules with twenty modules in total. Figure 2.6 shows a linear relationship between the cost and the value of output power. The initial cost of each two panels connected in series that give 0.560kW is \$1,745, replacement cost is \$1,342, and operational and maintenance cost is \$52 while the initial cost of 1.12kW is \$3,490, replacement cost is \$2,684. The PV system operates at MPPT which is chosen in HOMER instead of no tracking system.

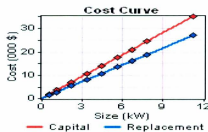


Figure 2.6: The cost curve of solar panel

### 2.3.3 Wind turbine

Two wind turbines from Bergey [40] Wind Power, of the model BWC-Excel-R/48, are used in this system. Each turbine has a rated capacity of 7.5kW and provides 48V DC. The technical parameters of this type of wind turbine are gathered from the data-sheets available from the company. A hub height of 30 meters is assumed for the proposed system. The HOMER software generated relationship (power curve) between the wind speed and the generated power is shown in figure 2.7. The cost breakdown for different turbine quantities including a capital cost of \$23,081, replacement cost of \$17,000, and annual operation and maintenance cost of \$462 is shown in figure 2.8 for one wind turbine. It is a linear relation between the cost and the quantity, the price is doubled when we have two wind turbines and so on. Wind data of 10m heights are used, the wind speed scaled up at Mulligan's telecommunication site is obtained as follows:

$$U_2 = U_1 \left( \frac{h_2}{h_1} \right)^\alpha$$

(2.1)

$U_2$  is scaled wind speed.

$U_1$  is wind speed data at highest  $h_1$ .

$h_1$  is hub height

$h_2$  is reference height

$\alpha$  is Shear exponent, which can be found by

$$\alpha = 0.096 \log(Z_0) + 0.016(\log Z_0)^2 + 0.24 \quad (2.2)$$

$Z_0$  is the highest value of the surrounding things (trees, houses,...)

Figure 2.9 shows the relation between the shear exponent and the highest value of the surrounding things.

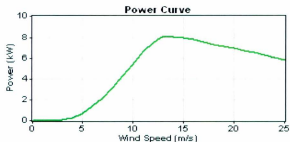


Figure 2.7: Wind turbine power curve

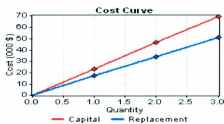


Figure 2.8: The cost curve of wind turbine

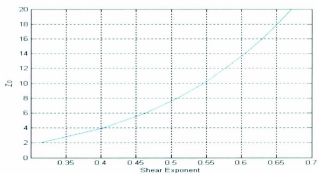


Figure 2.9: Shear exponent vs  $Z_0$

### 2.3.4 Diesel generator

The first non-renewable source in this system is the Perkins 404C-22G diesel generator. This generator runs at 1800rpm and is used to deliver AC power to the system through the inverter. This generator has a capacity of 20kW. The initial capital cost is \$16,308, the replacement cost is \$13,590, and operational and maintenance cost is \$0.1/hr, which are shown in figure 2.10. For this site the diesel can only be transported by air using a helicopter. Therefore the cost of the diesel together with its transportation cost is approximately \$5 per liter. The manufacturing efficiency chart is shown in figure 2.11 and fuel consumption data for the generator are shown in table 1. The diesel generator is used as a backup when the wind/PV system is unable to produce sufficient power for the load.

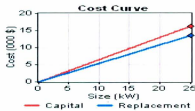


Figure 2.10: The cost curve of diesel generator

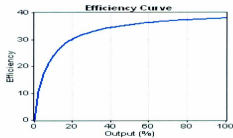


Figure 2.11: Efficiency Curve

Table 2-3: Consumption Data

Output Power (Kw)	Fuel Consumption (L/hr)
20	5.4
15	4
10	2.9

### 2.3.5 Battery bank

Two strings of VRLA GNB XL3000 batteries are used at Mulligan village and each battery is 2V and has a capacity 3000Ah with 48V total bus voltage. These batteries are replaced every 10 years. The initial capital cost, replacement cost, and maintenance and operation cost of all batteries are \$86,000, \$60,000, and \$100 respectively and the battery cost curve is shown in figure 2.12. The relation between the cost and the quantity is linear.

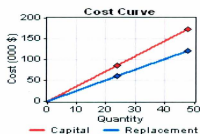


Figure 2.12: The cost curve of battery

### 2.3.6 Power converter

A converter is included in order to maintain the flow of energy between the AC and the DC bus. The conventional load is DC type, but generated power from the diesel generator is AC type. The size of the converter that is used in this system is 7kW. The initial capital cost and replacement cost are \$2,500 and \$1,500 respectively shown in figure 2.13. The relation between the cost and the output value of the converter is linear.

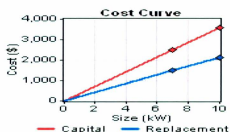


Figure 2.13: The cost curve of converter

## 2.4 System Optimizations

The non-renewable energy system (existing system) and the renewable energy system (proposed system) are simulated in HOMER software. The system cost and output are the considered factors for the optimization procedure. Analysis of the simulation results is presented below.

### 2.4.1 The existing system

The existing system architecture is shown in figure 2.14 and consists of a diesel generator and batteries to power the load. A Perkins 404C-22G diesel generator with

25kW at 1800rpm is used and the engine is rebuilt every 15,000 hours. Two strings of VRLA GNB XL3000 batteries are used at Mulligan village and each battery is 2V and has a capacity 3000Ah with 48V total bus voltage. These batteries are replaced every 10 years. A converter is included in order to maintain the flow of energy between the AC and the DC bus. The size of the converter that is used in this system is 7kW.

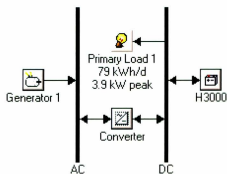


Figure 2.14: Existing power system at Mulligan

#### 2.4.2 The proposed system

The proposed hybrid renewable energy system is shown in figure 2.15, and consists of the existing power system, a wind turbine, and a photovoltaic panel. The proposed system will reduce diesel fuel consumption and the associated operation and maintenance cost. In this system the wind turbines and PV will be the primary power source and the diesel generator will be used as a backup for long term storage systems and batteries for short term storage systems.

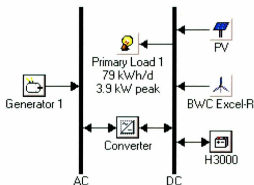


Figure 2.15: Proposed hybrid power system for Mulligan

## 2.5 Optimization and Comparison Results

Both systems were simulated in HOMER software, and the optimal results were obtained for each case. Moreover, the comparison of both systems was based on the pre-feasibility, electrical production, and emissions for each system, determined using HOMER software. The first system is a non-renewable energy system (the existing system) and the second is a renewable energy system (proposed system). These systems are designed to provide uninterrupted power for a telecommunication tower on a remote site. The diesel generator and the batteries that are used in both designs are the same model.

### 2.5.1 The existing system

Table 2.4 shows the optimized result for the non-renewable energy system. As shown in the figure, the Total Net Present Cost (TNPC) is \$823,072. The diesel generator burns 12,672L/Y of fuel per year and the annual generator run time is 1,536 hours. In twenty years the diesel generator will burn  $12,672\text{L/Y} \times 20\text{Y} = 253,440\text{L}$  of fuel. For this

site the diesel fuel can be transported only by helicopter. Therefore, the total cost of diesel fuel at \$5 per liter (high delivery cost) is very high. The probability of a fuel price increase is also high. The total cost is calculated with a constant price of fuel, which is \$5 per liter. The total fuel cost during these 20 years will be  $253,440L * 5\$/L = \$1,267,200$  and the total cost for the whole system will be  $\$1,267,200 + \$823,072 = \$2,090,272$ .

**Table 2-4: Optimized result for the non-renewable energy system**

Sensitivity Results | Optimization Results |

Double click on a system below for simulation results.

	Label	H3000	Conv. (kW)	Initial Capital	Operating Cost (\$/yr)	Total NPC	CDE (\$/kWh)	Ren. Frac.	Diesel (L)	Label (hrs)
	25	48	25	\$187,237	65,172	\$823,072	2.973	0.00	12,672	1,536

### 2.5.1.1 Electrical production

Figure 2.16 shows the monthly average electric production of the system from the HOMER simulation. As shown in the figure, all the electricity is produced by the diesel generator. The diesel generator's production of electricity depends on the load demand.

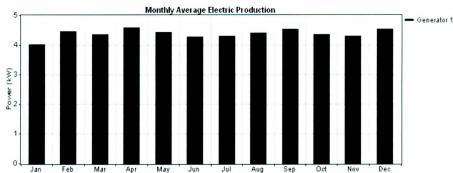


**Figure 2.16: Monthly average electric production for non-renewable energy system**

### 2.5.1.2 Emissions

The energy industry is the major cause of global emissions and is responsible for 40% of global CO<sub>2</sub> production. The transportation industry is responsible for 24%. Recent studies have shown that the communication industry is responsible for 2% of global CO<sub>2</sub> production in [41] and [42]. The emission of carbon dioxide is 33,370kg/yr, and the emission values of different gases are shown in table 2.5.

**Table 2-5: Emission values in the existing system estimated by from HOMER tool**

Pollutant	Emissions (kg/yr)
Carbon dioxide	33,370
Carbon monoxide	82.4
Unburned hydrocarbons	9.12
Particulate matter	6.21
Sulfur dioxide	67
Nitrogen oxides	735

### 2.5.2 The proposed system

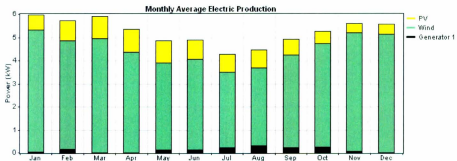
The renewable energy based system was also simulated in HOMER software with four sensitivity variables. These variables are wind speed, solar irradiation, load, and diesel price and each of these variables has three different values. Therefore, 81 sensitivity cases have been tested for the system. Table 2.6 shows the optimized results for the proposed system. The Total Net Present Cost (TNPC) is \$1,011,514. The system will consume only 335 liters of diesel fuel per year and the annual generator run time is expected to be 145 hours. The lifetime of this system is 25 years, but a 20 year life is used to make the comparison between the two systems. In twenty years the diesel generator will burn 6,700L of fuel and it will cost \$33,500. The total cost of the system will be around \$1,045,014.

**Table 2-6: Optimized result for the renewable energy system**

Sensitivity Results		Optimization Results										
Sensitivity variables												
Priority Load 1 (kWh/d)	79.1	Global Solar (kWh/m <sup>2</sup> /d)	2.05	Wind Speed (m/s)	6.26	Diesel Price (\$/L)	5					
Double click on a system below for simulation results.												
	PV (kW)	XLR (kW)	Label (kW)	H3000	Conv. (k/w)	Initial Capital	Operating Cost (\$/yr)	Total NPC	COE (\$/kWh)	Ren. Fac.	Diesel (L)	Label (hrs)
	5.60	2	25	24	7	\$968,420	4,150	\$1,011,514	3.305	0.90	335	145
		3	25	24	7	\$974,051	4,135	\$1,016,906	3.403	0.90	349	151

### 2.5.2.1 Electrical production

Figure 2.17 shows the monthly average electric production of the system. Photovoltaic production is 14% with 6,403kWh/yr. Diesel generator production is 2% with 1,052kWh/yr. Finally, the wind turbine is expected to supply the rest of the load which is 84% with 38,325kWh/yr, as shown in table 2.7.

**Figure 2.17: Monthly average electric production for renewable energy system****Table 2-7: Energy production for proposed system from HOMER software**

Production	kWh/yr	%
PV array	6,403	14
Wind turbines	38,325	84
Generator 1	1,088	2
Total	45,815	100

Figures 2.18, 2.19, and 2.20 show the yearly wind turbine output power spectrum, yearly PV output power spectrum, and yearly diesel generator output power spectrum respectively. The maximum power production from wind is 18kW, PV is 6.30kW, and 8kW is from the diesel generator. Most importantly, wind and solar energy sources do not need any backup from the diesel generator. In the months of March, April, and December, the diesel generator electrical production is almost zero watts.

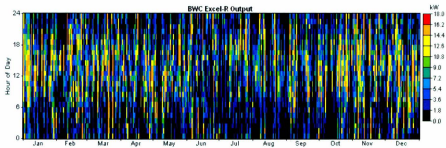


Figure 2.18: Yearly wind turbine output power spectrum from HOMER simulation

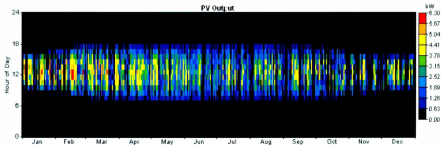


Figure 2.19: Yearly PV output power spectrum from HOMER simulation

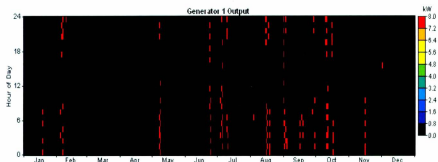


Figure 2.20: Yearly diesel generator output power spectrum from HOMER simulation

33.4% of the energy produced by the proposed system is excess electricity, 15,323kWh/yr . This amount of electricity would to reduce the grid cost if the system is grid connected, but this system is a stand-alone system. The excess electricity and renewable fraction values are shown in table 2.8.

Table 2-8: Excess energy for proposed system from HOMER software

Quantity	kWh/yr	%
Excess electricity	15,323	33.4
Unmet electric load	0.00	0.0
Capacity shortage	0.00	0.0
Quantity	Value	
Renewable fraction	0.976	

### 2.5.2.2 Emissions

The most environmentally friendly system is a system that has fewer carbon emissions, because carbon emissions are mainly responsible for environmental pollutions. Therefore, unwanted emissions will decrease by using integrated renewable energy

systems. Table 2.9 shows the emission values of different gases for the proposed system which are produced by the HOMER simulation tool.

**Table 2-9: Emission values in the proposed system estimated by HOMER tool**

Pollutant	Emissions (kg/yr)
Carbon dioxide	883
Carbon monoxide	2.18
Unburned hydrocarbons	0.241
Particulate matter	0.164
Sulfur dioxide	1.77
Nitrogen oxides	19.4

## 2.6 Summary

In this chapter, the simulation analysis of the existing and proposed hybrid system is done using the HOMER simulation tool to compare between both systems and to find the optimal sizing of the proposed system. HOMER software is available at the American National Renewable Energy Laboratory (NREL). Both systems are designed for off-grid application to provide uninterrupted power for a telecommunication site at a remote area in the Labrador region of Canada as presented in this research. The essential data has been obtained from BellAliant Company, NASA, with other data obtained from different companies. The capital cost, replacement cost, and Operation & Maintains (O&M) cost are obtained from different sources and assigned for each component. Moreover, sensitivity analysis is considered for different parameters (wind speed, solar irradiation, diesel prices, and primary load) to get the highest system performance. Subsequently, a comparison between the two systems is presented in this chapter which has three main factors. Firstly, the proposed system cost is less than the existing cost by \$1,045,258

which is a very significant number for a small system. Secondly, the electrical production in two systems is very big different. Diesel generator run times are reduced, and the diesel generator in the proposed system will produce only 2% of the total power production. Moreover, the diesel generator will require less maintenance and operation cost and a longer period of service before a replacement. Finally, the important comparison subject is emissions. As is known, carbon dioxide is the main cause of global warming. 33,370kg/yr of carbon dioxide is produced from the existing system while 880kg/yr will be produced from the proposed system.

## Chapter 3 Modeling of Hybrid Power System

### 3.1 Primary Energy Sources

Electrical energy systems can be one of three types; static, rotating, or energy storing. This difference in the systems depends on the primary sources, whether they are stand-alone or grid connected, and the cost of system output [43]. The largest energy resource available to the earth is the sun which can provide 15,000 times more energy than the total use of fossil and nuclear fuel during one year [44]. Canada is a world leader in the production and use of energy from renewable resources. These resources include moving water, biomass, wind, solar, geothermal and ocean energy. The most used renewable energy source in Canada is hydro while wind and solar sources are experiencing a high growth rate. For the Mulligan telecommunication site, wind and solar are the most suitable energy resources to provide an uninterrupted power. A photograph of BellAliant's telecommunication site at Mulligan, Labrador is shown in figure 3.1 [45].



Figure 3.1: A photograph of Bell-Aliant's telecommunication site at Mulligan, Labrador

### 3.2 Wind Energy System

Wind energy technology is the most promising among the renewable energy technologies to produce electricity at remote sites. The use of wind energy conversion systems (WECS) is experiencing a high growth rate worldwide. The following section provides modeling of the wind energy conversion system.

#### 3.2.1 Energy in wind

Wind energy is kinetic energy of the wind, converted into electrical energy or used in some other way. The kinetic energy  $E$  of any particular mass  $m$  of moving air at speed  $v$  in (m/s) can be expressed as [46], [1], and [47].

$$E = \frac{1}{2}mv^2(\text{Joules/sec}) \quad (3.1)$$

The kinetic energy is received by wind turbine blades in cross section area  $A$  in ( $\text{m}^2$ ) at speed  $v$ . The mass of air passing through this area is obtained by:

$$m = \rho Av \quad (3.2)$$

where  $\rho$  is the air density ( $\text{kg}/\text{m}^3$ ).

The wind power  $P_w$  based on the above two equations is

$$P_w = \frac{1}{2}\rho Av^3 \quad (3.3)$$

Wind power cannot be fully converted to mechanical power. So, the wind turbine output power can be calculated by the following equation:

$$P_m = C_p P_w$$

$$P_m = \frac{1}{2}\rho AC_p v^3 \quad (3.4)$$

Typically, the air density is taken as  $1.225\text{kg/m}^3$ .  $C_p$  is called the power coefficient of the rotor or the rotor efficiency, which is useful as it is the only variable and controllable parameter. The  $C_p$  is a ratio of wind turbine output mechanical power  $P_m$  to power of wind  $P_w$  and it is a function of tip speed ratio  $\lambda$  and pitch angle  $\beta$ .

### 3.2.2 Tip speed ratio

Tip speed ratio  $\lambda$  (TSR) is the ratio of the rotational speed  $\omega$  of the wind turbine to the linear wind speed  $v$  at the tip of the blades. It can be expressed as follows [47-49]:

$$\lambda = \frac{\omega R}{v} \quad (3.5)$$

where  $R$  is the wind turbine rotor blade radius in  $m$ .

The tip speed ratio is related to the wind turbine operating at its maximum power, and the maximum coefficient power can be achieved at a particular TSR value, which is typically about 6. For variable TSR values, the rotor speed will change to keep the TSR at an optimum level.

### 3.2.3 Wind turbine output power vs. wind speed

A typical wind turbine power curve is shown in figure 3.2. Once the wind speed reaches the cut-in wind speed which is the speed where the turbine starts generate a useful power. The wind turbine power output is changeable between the cut-in and rated wind speed, which is normally 11-15m/s. The wind turbine produces maximum power between the rated and cut-out wind speed. If the wind's speed is greater than the nominal value, the wind turbine maintains the same output power. However, if the wind speed is higher than the cut-out wind speed, the wind turbine is automatically put out of production for

protection of its components. No power is produced before cut-in or after cut-out wind speed and the needed power of each wind turbine is given at the rated wind speed [1, 50].

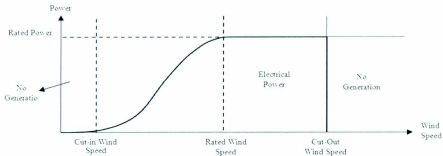


Figure 3.2: A typical wind turbine power curve

### 3.2.4 Wind energy conversion system

The schematic diagram of a typical wind energy conversion system is shown in Figure 3.3. The wind power system is a combination of different units, and the principal components of the modern wind turbine are:

- The Tower
- Rotor Blade
- Rotor Shaft and Bearing
- The Yaw Mechanism
- The Mechanical Gear
- The Electrical Generator
- The Speed Sensors and Control
- The Power Electronics

- Battery for a Stand-Alone
- Transmission Link Connecting to the Grid

The tower holds the main components of the wind turbine, such as: blades, rotor, gear box, generator, controller, yaw drive, yaw motor, etc. The yaw mechanism is used to move the blades into the wind direction. In the wind power system, the rotor blades capture the kinetic wind energy which goes to the gearbox and transforms the slower rotational speed of the wind turbine to a higher rotational speed at the electrical generator. The electricity is generated when the wind turbine drives the electrical generator shaft.

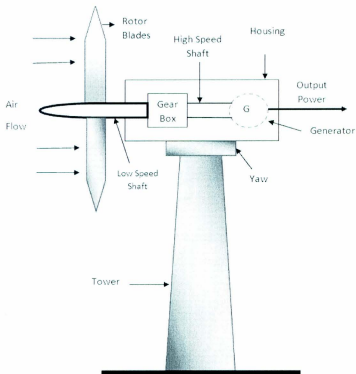


Figure 3.3: Schematic diagram of wind energy conversion system

### 3.2.5 Types of wind turbines

There are many categories of wind turbines. Two different types may be distinguished depending on the rotor orientation as shown in this section: upwind turbine and downwind turbine. In the upwind turbine the rotor is located in front of the tower, while the downwind turbine rotor is located behind the tower. In other words, the rotor is facing the wind in the upwind speed type while in the downwind type the rotor is downwind. Figure 3.4 shows both types of wind turbines. In the proposed system, the upwind turbine was used.

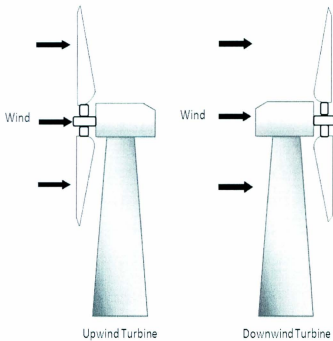


Figure 3.4: Upwind and downwind type wind turbines

### 3.2.6 Modeling and simulation of Bergey wind turbine

Two BWC-Excel-R/48 are used in the proposed hybrid system and each turbine has a rated capacity of 7.5kW and provides 48V DC. The Bergey Excel 7.5 wind turbine block diagram dynamic model is shown in Figure 3.5. The wind turbine is a permanent magnet generator (PMG) based wind turbine. Some power electronic devices are needed in the model such as: the universal bridge, used to convert the three phase AC to one phase DC. The Pitch angle is kept at zero (no pitch control) in this model and the generator speed is fed back from the permanent magnet generator. The measured tip speed ratio is compared to the actual tip speed ratio which has a value of 6 as in the wind turbine specifications. Then, the difference of error between the tip speed ratios is connected to the PID controller. The further specifications obtained from [40] are given in table 3.1. The subsystem model is shown in appendix A-1.

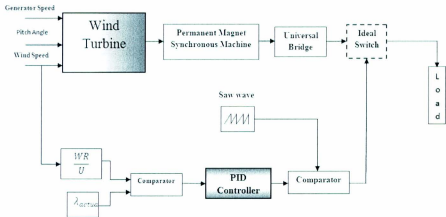


Figure 3.5: System block diagram of WECS

**Table 3-1: Beregy Excel 7.5 wind turbine specifications**

<b>Parameters</b>	<b>Specifications</b>
Start-up Wind Speed	3.4 m/s (7.5 mph)
Cut-in Wind Speed:	2.5 m/s (5 mph) – grid intertie; 4 m/s (9 mph) – battery charging
Rated Wind Speed	12 m/s (27 mph)
Rated Power	7.5 kW for battery-charging
Cut-Out Wind Speed	None
Furling Wind Speed	15.6 m/s (35 mph)
Max. Design Wind Speed	60 m/s (134 mph)
Type	3 Blade Upwind
Rotor Diameter	7 m (23 ft.)
Blade Pitch Control	None, Fixed Pitch
Over-speed Protection	AUTOFURL
Gearbox	None, Direct Drive
Temperature Range	-40 to +60 Deg. C
Generator	Permanent Magnet Alternator
Output Form	3 Phase AC, Variable Frequency

The Simulink modeling of the wind turbine is given in Appendix A. The wind turbine power curve obtained from the Simulink is shown in figure 3.6. The rated wind speed is 12m/s which gives the rated power of 7,500W, which keeps the output power constant if

the wind speed is greater than the rated wind speed. The output powers from the wind energy conversion system for four different wind speeds are given in figure 3.7.

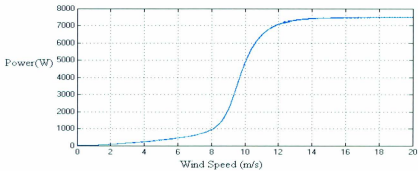


Figure 3.6: Wind turbine power curve

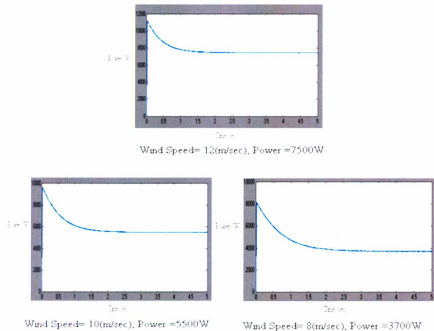


Figure 3.7: WECS output power for different wind speeds

### 3.3 Solar Energy System

The idea of solar cells started in 1839. Edmund Becquerel discovered the photovoltaic effect when light was shone on an electrode in an electrolyte solution. In 1877, William Adams and Richard Day made a selenium solar cell which reached about 1% efficiency by 1914. Semiconductor solar cells were first produced in 1954 with 6% efficiency [51]. Renewable energy was considered by the majority of industrialized countries after the OPEC oil embargo in 1973-1974. Nowadays, the Photovoltaic cell is the fastest growing power generation technology and it is widely used. Figure 3.8 shows the World total PV cells installed capacity from 1996 to 2010 in [5, 52].

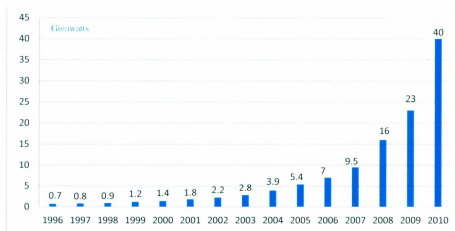


Figure 3.8: The World total PV cells installed capacity(5)

#### 3.3.1 The fundamentals of PV

The solar cell is a semiconductor p-n junction device which converts solar energy to electrical energy through the PV effect. Figure 3.9 illustrates the principle of a p-n

junction solar cell. The sunlight hits the p-n junction device; light photons with certain wavelengths (energy greater than the band-gap energy of the semiconductor) are absorbed by the semiconductor material and generate electrons and holes. Electrons from the n-region close to the junction flow to the p-region and leave a positively charged layer, while holes flow to the n-region and leave a negatively charged layer. There is an electric field acting as a guide for the electron flows at the junction between two regions, which is called a p-n junction. As shown in figure 3.9, the electrons flows out of the n-region, go to the load, and then back to the p-region. The current flows in the opposite direction from the electrons [53, 54].

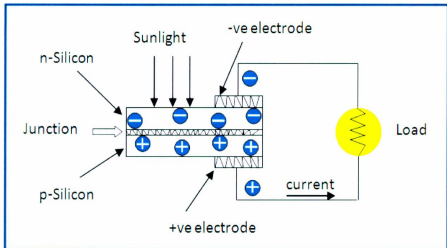


Figure 3.9: An illustration of p-n junction solar cell(53)

### 3.3.2 Photovoltaic modeling

A solar cell module is the basic element of the photovoltaic system. The solar cell model consists of a diode, a current source, a series resistance and a parallel resistance, as

shown in figure 3.10. The energy variables for the solar system are radiation and temperature. Equation (3.6) shows an expression for the solar module. It is a function of solar radiation and ambient temperature. The diode is used to represent the p-n junction of the solar cell [6].

$$I = I_{ph} - I_S [\exp \{q(V + IR_s)/(KT_C A)\} - 1] - [(V + IR_s)/R_{SH}] \quad (3.6)$$

where:

$I$  is cell output current,  $V$  is cell output voltage,  $I_S$  is saturation current,  $q$  is electronic charge ( $0.6039 \exp^{-19} C$ ),  $R_s$  is a series resistance,  $K$  is Boltzmann's constant ( $1.38 \exp^{-23} J/K$ ),  $T_C$  is cell temperature,  $A$  is an ideal factor ( $=1.740$ ), and  $R_{SH}$  is a shunt resistance (parallel resistance= $\infty$ ). The photocurrent mainly depends on solar insolation and the cell's working temperature, which is described as:

$$I_{ph} = [I_{SC} + K_t(T_C - T_{Ref})] \lambda \quad (3.7)$$

where:

$I_{SC}$  is short circuit current,  $K_t$  is the short-circuit current temperature coefficient ( $A/C$ ).  $T_{Ref}$  is the room temperature  $25^\circ C$ , and  $\lambda$  is a solar irradiation in  $W/m^2$ . The cell's saturation current is described as:

$$I_S = I_{RS} (T_C/T_{Ref})^3 \exp [qE_G (\frac{1}{T_{Ref}} - 1/T_C)/kA] \quad (3.8)$$

where:

$I_{RS}$  is the cell's reverse saturation current,  $E_G$  is the band gap for silicon (i.e.  $1.12 eV$ ).



Figure 3.10: Solar cell model

### 3.3.3 Photovoltaic module and array

The module is a combination of several cell strings that are connected together in parallel. Each string contains several cells connected in series. Most PV modules have either 36 or 72 solar cells with bus voltage of 12V or 24V. The PV array is a combination of several modules in parallel and series, and the way they connect depends on the bus voltage and output power that needs to be produced. Figure 3.11 shows the PV cell, module and array [54].

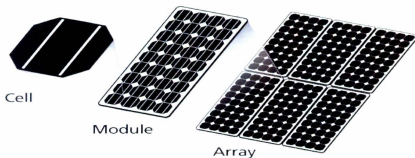
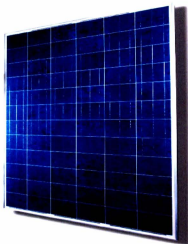


Figure 3.11: PV cell, module and array [59]

The module used in our system is shown in figure 3.12, which contains 6 strings. Each string contains 12 cells with a total of 72 solar cells. This module produces 280W maximum power and 24V bus voltage [56].



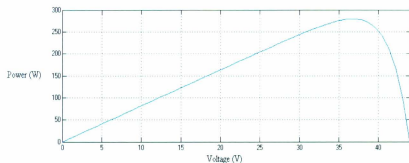
**Figure 3.12: PV Module STP280-24V [60]**

### **3.3.4 Photovoltaic model in Matlab/Simulink**

Two PV modules are connected in series to meet the bus voltage which is 48V. The 6.5kW PV rated capacity is used in this system, connected in 10 strings. Each one has two modules with twenty modules in total. Based on equation 3.6, a dynamic model for a PV cell has been developed in Matlab/Simulink, and the PV module is modeled the same way. The only difference is the voltage parameters. The model specification parameters are given in table 3.2 [56]. P-V output characteristics with 1000(W/m<sup>2</sup>), 800(W/m<sup>2</sup>) and 600(W/m<sup>2</sup>) radiation intensity and 25°C ambient temperature are shown in figure 3.13, 3.14 and 3.15 respectively. The subsystem model is shown in appendix A.

Table 3-2: The PV model parameters

Parameters	Specifications
Optimum operating voltage ( $V_{mp}$ )	35.2 V
Optimum operating current ( $I_{mp}$ )	7.95 A
Open-Circuit Voltage ( $V_{oc}$ )	44.8 V
Short-Circuit Current ( $I_{sc}$ )	8.33 A
Maximum Power at 1000 W/m <sup>2</sup> irradiation	280 W
Module Efficiency	14.4%
Operating Module Temperature	-40° C to +85° C
Maximum System Voltage	600 V DC (UL)/1000 V DC (IEC)
Maximum Series Fuse Rating	20 A
Power Tolerance	0/+5 %
Solar Cell	Polycrystalline 156*156 mm (6 inches)
No. of cells	72 (6*12)

Figure 3.13: P-V output characteristics with 1000 W/m<sup>2</sup>

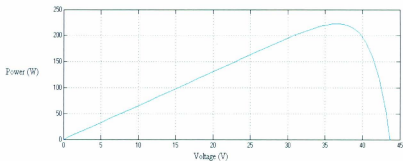


**Figure 3.14: P-V output characteristics with 800(W/m<sup>2</sup>)**

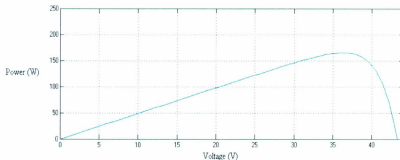


**Figure 3.15: P-V output characteristics with 600(W/m<sup>2</sup>)**

### 3.3.5 Maximum power point tracking

The photovoltaic module is made up of very expensive material (silicon cells) and, as is known, the efficiency of solar cells is low (around 13%). Therefore, it is very desirable to operate the PV module at the peak power point. Maximum power point tracking (MPPT) is one of the techniques that are used to obtain the maximum power from the PV module. In recent years many researchers have developed maximum power point tracking techniques. The only difference in all these studies is the controller used in MPPT

techniques in [57],[58],[59], and [60]. Figure 3.16 shows P-V output characteristics with 1000(W/m<sup>2</sup>) radiation intensity and 25°C ambient temperature with the MPPT technique while figure 3.17 shows the effect of solar irradiance.

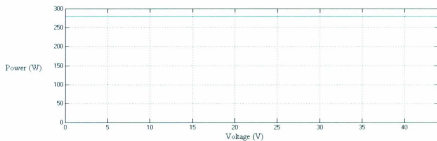


Figure 3.16: P-V output characteristics with MPPT technique

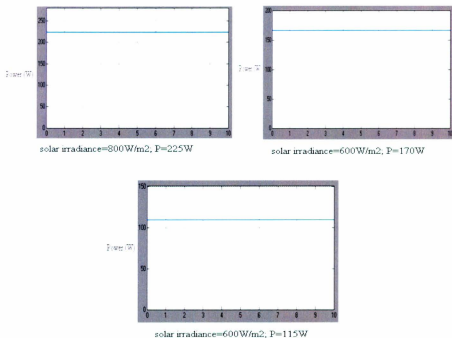


Figure 3.17: The effect of solar irradiance

### 3.4 Diesel Generator

Although the diesel generator has emissions, it is widely used in power systems. It is the main power source for off grid applications, and is used as a backup for grid applications without connecting to the grid. Diesel generators can be shipped anywhere, but the initial shipping cost is very high when the generator is delivered to remote areas. In addition, the fuel cost will be very high to transport generators to a remote area. In our system, the main purpose of the diesel generator is to use as a backup energy source when the renewable resources under-perform. Figure 3.18 shows a diesel generator with 20kW developed in Matlab/Simulink and figure 3.19 shows the engine and excitation system of the diesel generator. The sizing results show energy production from the generator is around 2% of the total power demand and figure 3.20 shows the simulation results of diesel production [6]. The subsystem model is shown in appendix A.

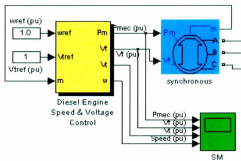


Figure 3.18: Diesel generator model in Matlab/Simulink

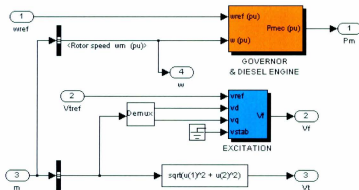


Figure 3.19: Engine and excitation system of diesel generator

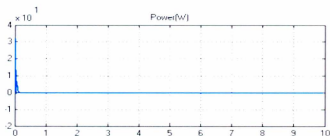


Figure 3.20: Diesel generator power curve

### 3.5 Energy Storage

Energy storage devices store electrical energy that can be used whenever there is a need to meet the demand. Energy storage devices can manage the amount of required power to meet the load demand, they can maintain a balance between the load and generation by providing frequency regulation to the grid, and they can be used as a backup with renewable energy for off grid applications. The battery is one of the most common energy storage technologies used in energy systems, which converts chemical

energy to electrical energy. There are different types of batteries; the most commonly used are: Lead/acid, invented in 1859 by Gaston Plante, and Ni-Cd is one of the oldest energy storage technologies. Other batteries like Ni-MH have no pollution compared with the first batteries, and Ni-MH has high a performance at the ambient temperature. Nickel-Zinc is mostly used in an alkaline environment [61]. The lead acid battery is used in our system as a backup for short term power storage. A battery model in Matlab/Simulink is shown in figure 3.21. Equations 3.9 and 3.10 express discharge and charge battery models respectively [62].

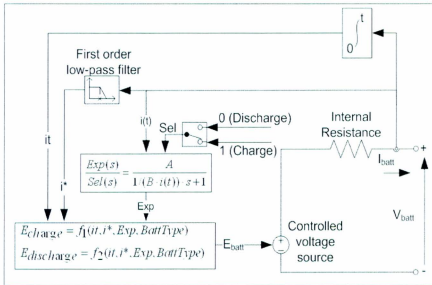


Figure 3.21: Battery model in Matlab/Simulink

Discharge model ( $i^* > 0$ )

$$E_{discharge} = E_0 - K \cdot \frac{Q}{Q - i^*} \cdot i^* - K \cdot \frac{Q}{Q - i^*} \cdot i(t) + \text{Laplace}^{-1} \left( \frac{\text{Exp}(s)}{\text{Sel}(s)}, 0 \right) \quad (3.9)$$

Charge model ( $i^* < 0$ )

$$E_{charge} = E_0 - K \cdot \frac{Q}{it + 0.1Q} \cdot i^* - K \cdot \frac{Q}{Q - it} \cdot it + Laplace^{-1} \left( \frac{Exp(s) \cdot \frac{1}{s}}{Sel(s)} \right) \quad (3.10)$$

where:

$E_{Batt}$  = Nonlinear voltage (V)

$E_0$  = Constant voltage (V)

Exp(s) = Exponential zone dynamics (V)

Sel(s) = Represents the battery mode. Sel(s) = 0 during battery discharge, Sel(s) = 1 during battery charging.

K = Polarization constant (Ah-1) or Polarization resistance (Ohms)

$i^*$  = Low frequency current dynamics (A)

$i$  = Battery current (A)

$it$  = Extracted capacity (Ah)

Q = Maximum battery capacity (Ah)

A = Exponential voltage (V)

B = Exponential capacity (Ah)

### 3.6 Summary

The wind energy conversion system, solar energy conversion system, diesel engine, and batteries employed in Mulligan are all described in this chapter. The simulation results of all system components are presented in this chapter as well. Wind and solar subsystems are used as a primary power source, while a diesel generator is used as a backup source for long term and the battery bank as a backup source for short term. The simulation results of a combined system will be presented in chapter 5.

## **Chapter 4 Experimental Testing of Proposed Supervisory Controller**

### **4.1 Introduction**

One of the most important factors in designing a hybrid power system is the design of the supervisory controller. The complexity of designing a hybrid system supervisory controller depends on the total number of components that need to be controlled. More components mean more complexity in designing the supervisory control. A test setup was built to test the proposed on/off type supervisory controller in the lab. This chapter provides details of the test setup and some test results. The developed application for monitoring and automatic control has been implemented for a hybrid power system consisting of a wind turbine subsystem, PV subsystem, power supply, and energy storage. A power supply is used instead of a diesel generator in the test setup. The experimental setup was developed for a hybrid power system smaller than Mulligan's system because of the unavailability of larger size equipment at Memorial University's Faculty of Engineering labs. However, the idea of the designed controller will be the same for both systems.

### **4.2 Experimental Setup**

A schematic diagram of the experiment setup is shown in figure 4.1. An Air-X wind turbine and Coleman solar panels are connected to the load through relays and current sensors. All power sources and the load are connected to the 12VDC lead acid battery. Two light bulbs were implemented in the experiment as a load. Each bulb light was 60W and 12 V. The supervisory controller makes decisions on which system should

be put on-line and which should be turned off. The supervisory controller connects the wind turbine first through the relay which is driven by the relay driver circuit. The supervisory controller monitors the current supplied by the wind turbine and the load current. If the wind turbine cannot handle the load demand, the controller will connect the PV. Also, if both sources cannot handle the load demand, the controller will disconnect the wind turbine and PV system and will connect the power supply for a certain time to charge a battery. The battery is considered as a load component in this case although it will maintain a stable voltage. Figure 4.2 shows the experimental setup in the Fluid Lab with various components. The experimental setup consists of the following components:

- i. Wind turbine
- ii. Wind Tunnel
- iii. Photovoltaic panels
- iv. Power supply
- v. Two Bulb lights
- vi. Battery
- vii. Three current sensors
- viii. Three electromechanical relays
- ix. Three relay driver circuits
- x. Microcontroller Board

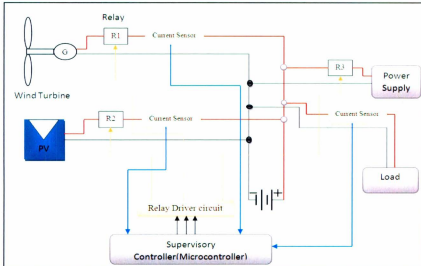


Figure 4.1: Schematic diagram of the experiment setup

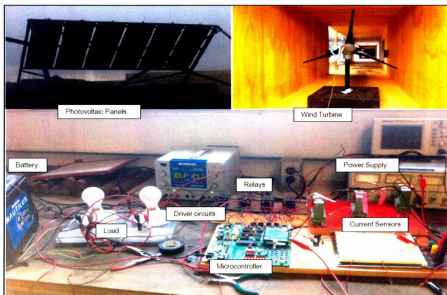


Figure 4.2: The experimental setup in the lab with various components

### 4.3 Wind Turbine

An Air-X wind turbine with a 400W rated power capacity from southwest wind power is used in the experiment. Then Air-X wind turbine is installed in the wind tunnel of the Fluid Lab at Memorial University. The wind speed in this tunnel is controllable which has the advantage of increasing and decreasing the wind speed as needed. The Air-X wind turbine in the tunnel is shown in figure 4.3 and specification parameters are given in table 4.1 in [67].



Figure 4.3: Air-X wind turbine in the wind tunnel

Table 4-1: Air-X wind turbine specifications

Parameters	Specifications
Start-up Wind Speed	3.58 m/s (8 mph)
Rated Wind Speed	12.5 m/s (28 mph)
Rated Power	400W
Max. Design Wind Speed	49.2 m/s (110 mph)
Type	3 Blade Carbon fiber composite
Rotor Diameter	1.15 m
Turbine Controller	Microprocessor-based smart internal regulator with peak power tracking
Over-speed Protection	Electronic torque control

Wind speed in the tunnel was measured and wind speed at the wind turbine was calculated as presented in table 4.2. The area where the wind speed is measured in the tunnel is different than the area where the wind turbine is located. A scale down is done by the following equation:

$$V_2 = V_1 * \frac{A_1}{A_2} \quad (4.1)$$

where:

$V_2$  is wind speed at where the wind turbine is in the tunnel

$V_1$  is wind speed at the middle of the tunnel

$A_1$  is the area at the middle of the tunnel

$A_2$  is the area at where the wind turbine is in the tunnel which is  $1.4 * 1.18 = 1.652 \text{m}^2$ .

**Table 4-2: Wind speed measurements**

Wind speed at the middle of the tunnel (m/s)	Blades rotational speed (rpm)	Wind speed where the wind turbine is in the tunnel (m/s)
7.9	185	4.78
10	971	6
12	1157	7.26
14	1446	8.5

#### **4.4 Photovoltaic Panel**

Coleman 120W solar panels are installed on the roof at the Faculty of Engineering, Memorial University. Three panels are connected together to provide 60W and six panels are installed with a total capacity of 120W in [68]. These panels have an MPPT charge controller and are connected to 12 VDC batteries. In the experiment, PV panels are considered as a second source of power for the hybrid power system. Solar panels on the roof are shown in figure 4.4.

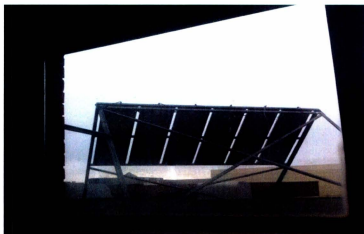


**Figure 4.4: Solar panels on the roof**

#### **4.5 DC Current Transducer (CR5210)**

The current transducer CR5210 is designed to provide a DC voltage signal which is proportional to a DC sensed current. The transducer can sense 50A DC current and provide 5V DC voltage. Three current transducers are used in the experiment to sense wind turbine current, PV panel current, and load current, and the transducers output is connected to the microcontroller board. CR5210 specification parameters are given in table 4.3 [65]. Figure 4.5 shows the CR5210 current transducers in the experiment setup while figure 4.6 shows the connection diagram of CR5210.

Table 4-3: Current transducer specifications

Parameters	Specifications
Basic Accuracy	1%
Operating Temperature	0°C to +50°C
Response Time	250 ms
Insulation Voltage	2500 VDC
Supply Voltage	24 VDC $\pm$ 10%
Frequency Range	DC only
Output Load	$\pm$ 5VDC

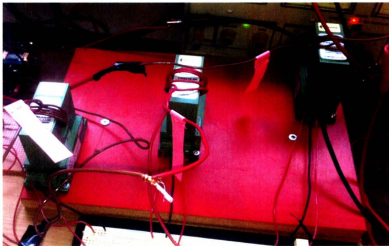


Figure 4.5: CR5210 current transducers

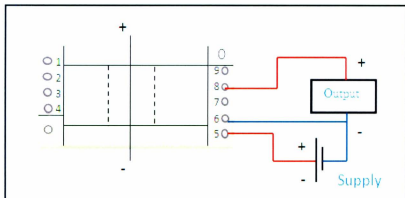


Figure 4.6: CR5210 connection diagram

#### 4.6 Electromechanical Relay

A relay is a switch which is operated by its control voltage. The relay has a coil, and when this coil is powered a magnetic field will be created and will operate a mechanical switch. The relay's coil current requirement is usually more than 100mA but a microcontroller cannot handle this much current. Therefore, a transistor is used in the relay driver circuit. A typical electromechanical relay used in the experiment is shown in figure 4.7 in [66].

Three 120/240 V AC relays are used in the experiment. These relays can handle a maximum current of 10A and can be operated by a 5V DC signal. The relays are used to connect and disconnect power sources: a wind turbine, photovoltaic panels, and a power supply.

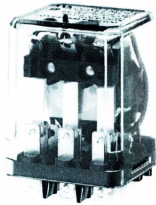


Figure 4.7: A typical electromechanical relay(66)

#### 4.7 Relay Driver circuits

Three driver circuits were used in the experiment to control the relays. These circuits are based on an NPN transistor, which works as a switch. The transistor was connected to the microcontroller via a 3.9Kohm resistor to make sure the relay stayed off when the microcontroller did not supply the 5V. The transistors are activated by the microcontroller signal which is 5V. A 1N4007 diode was connected in reverse bias across the relay's coil to protect the transistor from the electromagnetic force (EMF) created when the relay was released from the energized or ON state. The schematic of the relay driver circuits are shown in figure 4.8 which was drawn by the Proteus program. Figure 4.9 shows the relays with their driver circuits that were used in the experiment.

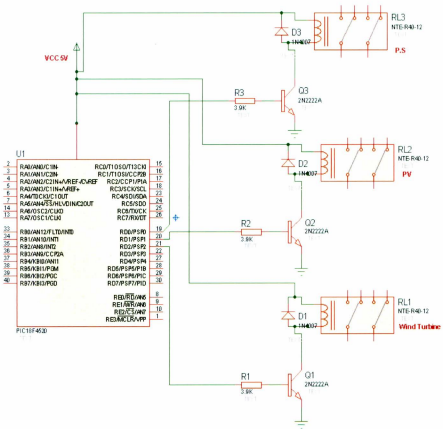


Figure 4.8: Relay driver circuits



Diagram of Human Body System

A detailed description of the diagram above, explaining the components and the system it represents. The diagram illustrates the human body system, showing the internal organs and the network of lines representing the system. The system is composed of several interconnected components, including the lungs, stomach, and intestines, which are connected by a network of colored lines. The blue line represents the main system, while the other lines represent the various components and their interactions. The diagram is a clear and concise representation of the human body system, showing the complex network of organs and their connections.

Table 4-4: PIC18F4520 specifications

<b>Parameters</b>	<b>Specifications</b>
Program Memory Type	Flash
Program Memory (KB)	32
CPU Speed (MIPS)	10
RAM Bytes	1536
Data EEPROM (bytes)	256
Digital Communication Peripherals	1-A/E/USART, 1-MSSP(SPI/I2C)
Capture/Compare/PWM Peripherals	1 CCP, 1 ECCP
Timers	1*8-bit, 3*16-bit
ADC	13ch, 10-bit
Comparators	2
Temperature Range (C)	-40 to 125
Operating Voltage Range (V)	2 to 5.5
Pin Count	40



Figure 4.10: EasyPic-4 used in the experiment

#### 4.9 Supervisory Controller

The supervisory controller supervises the overall system performance and generates the appropriate signals. For any remote power system, the interconnections between the equipment need to be monitored and controlled automatically due to the difficult and costly site access. The target of the controller is to keep the system running at an operating point where if any failure occurs, the controller will have enough time to take a counter measure. Depending on the control algorithm, a number of input signals were measured. In the experiment, there were three input signals: wind turbine current, PV current, and load current. They were sensed by current transducers and the outputs of the transducers were connected to the microcontroller. Based on the transducers output, the PIC18F4520 would manage and automatically control the system components. The schematic diagram of the supervisory controller implemented in the experiment is shown

in figure 4.11 while the flow chart of the supervisory controller is shown in figure 4.12.

The PIC was programmed by the mikroBasic and the program is shown in appendix B.

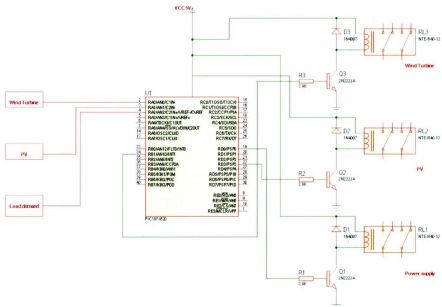


Figure 4.11: Schematic diagram of the supervisory controller

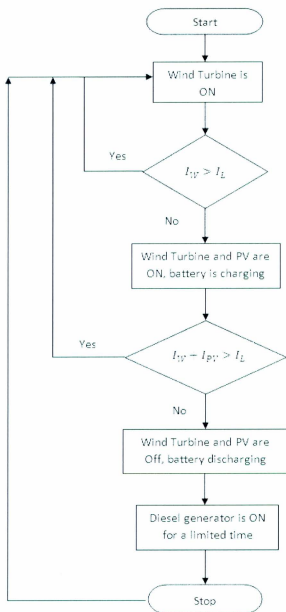


Figure 4.12: Supervisory controller flow chart

#### **4.10 Summary**

The experimental setup components are explained in this chapter. The main objective of this chapter is to explain the supervisory controller and how it works. A supervisory controller with a simple design is presented, which consists of a PIC18F4520 microcontroller, current transducers, relays, and relay driver circuits. In addition, positive results have been obtained with this simple controller and these are explained in the next chapter.

## Chapter 5 Results and Discussion

### 5.1 Introduction

Optimal sizing and a pre-feasibility study of the off-grid energy system configurations for powering a telecommunication site at a remote area in Labrador, the Mulligan telecommunication site, is presented in this research. The sizing and prefeasibility are done by HOMER software. The results are presented in Chapter 2 in detail. Dynamic modeling of the system is done by MATLAB/SIMULINK and the results are presented in the next section. Finally, the results of the real time supervisory controller are presented. As mentioned in chapter 4, the experiments were done for a small scale system, which is smaller than the Mulligan system.

### 5.2 Modeling Results

The system configuration of the proposed alternative hybrid energy system is shown in figure 5.1. This proposed system was implemented in MATLAB/SIMULINK to investigate the performance. The model includes two 7.5kW wind turbines, a 5.6kW PV, 20kW diesel generator, and a 48V battery bank. All of these components are connected to the load and the dump load to power and control the system. The load size results are presented in figure 5.2 comprised of current, voltage and power from the overall output. The variation here is very low because the site has the same load profile daily. Several different scenarios are done in the modeling part. Firstly, the wind speed input is a step response with 10m/sec initial value to 12m/sec final value when the step time is 2. Therefore, the power changes from 3.05kW when the wind speed is 10m/sec to 3.25kW

when the wind speed is 12m/sec. Figure 5.3 shows the current, voltage and power when the wind speed changes from 12m/sec to 14m/sec. The MATLAB/SIMULINK combined system is shown in appendix A.

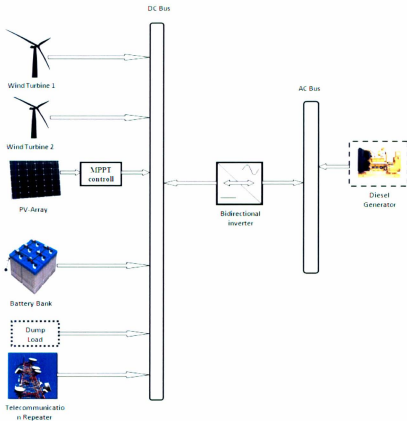


Figure 5.1: System configuration of the proposed alternative hybrid energy system

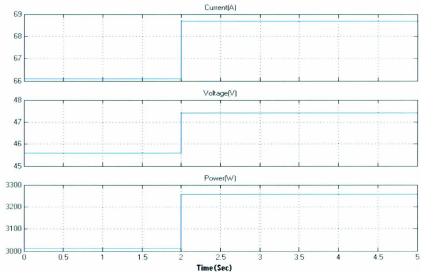


Figure 5.2: Current, voltage, and power of the system 10m/s to 12m/s wind speed

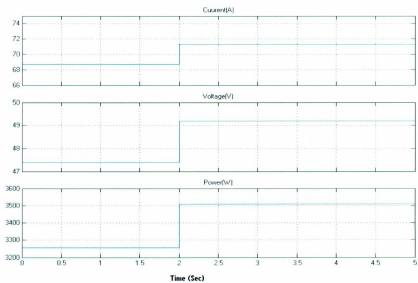
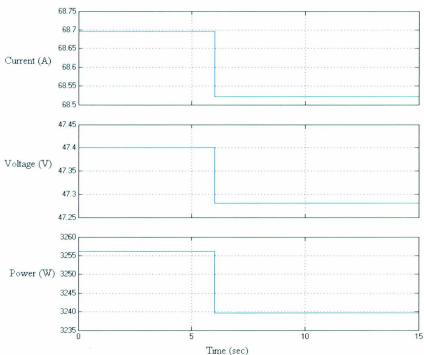


Figure 5.3: Current, voltage, and power of the system 12m/s to 14m/s wind speed

Secondly, the solar irradiance changes from  $1000\text{W}/\text{m}^2$  to  $800\text{W}/\text{m}^2$  and figure 5.4 shows the output current, voltage and power of the system.



**Figure 5.4: Current, voltage, and output power of the system  $1000\text{W}/\text{m}^2$  to  $800\text{W}/\text{m}^2$  solar irradiance**

Finally, different loads have been tested in this system. Figure 5.5 shows the system output when the load is increased while figure 5.6 shows the system output when the load is decreased.

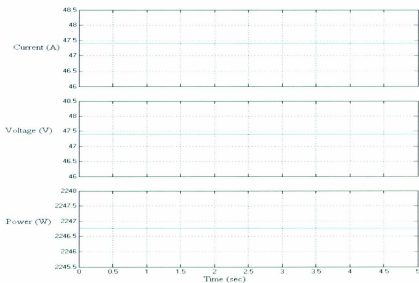


Figure 5.5: The system output when the load is increased

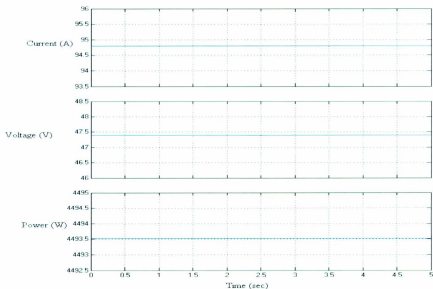


Figure 5.6: The system output when the load is decreased

### **5.3 Experiment Results**

Two bulb lights were used in the experiment as a load. Each bulb light has 60W and 12 V. Three cases are tested in this experiment: sunny day, cloudy day, and no wind.

#### **5.3.1 Case study 1**

The first case study was implemented for 70 minutes to monitor the battery state of charge. The battery was fully charged at the beginning. The results are presented in this chapter for three different times.

##### **5.3.1.1 Case study 1 in first 7 minutes**

First, the experiment was carried out on a sunny day, with wind speed around 8m/s. The results of the wind turbine output current, PV output current, load demand, battery state of charge, and diesel generator status are shown in Table 5.1. From time to time the wind speed was decreased, and immediately the diesel (power supply) was turned ON for a minute to meet the load demand. The battery was kept at the same level of charging, was increased when the wind and PV were on, while it was discharging when the wind and PV were off and the power supply was ON. The PV output current, wind output current, and battery state of charge for the first seven minutes are shown in figures 5.7, 5.8, and 5.9 respectively.

The wind turbine at Memorial University was installed in the wind tunnel at the Fluid lab in the tunnel. The wind speed in this tunnel is controllable, which has the advantage of increasing and decreasing the wind speed as needed. On the other hand, the wind turbine in this tunnel has some disadvantages, as it is not fixed well in the tunnel and moves from

right to left (yaw) a little bit. The table below shows the wind output current changes from 4.41 to 4.60A. This movement in the wind turbine makes some problems for the controller.

**Table 5-1: Experiment results in first 7 minutes**

Time (minutes)	Battery Voltage (V)	Load Current (A)	PV Current (A)	Wind Current (A)	Diesel generator
1-3	12.16 v	7.72	2.38	4.47 (4.41-4.60)	off
3-4	12.14 discharging	7.69	0	0	on
4-7	12.16 v	7.72	2.38	4.47 (4.41-4.60)	off

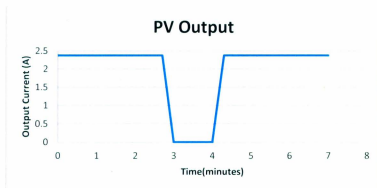


**Figure 5.7: PV output current in first 7 minutes**

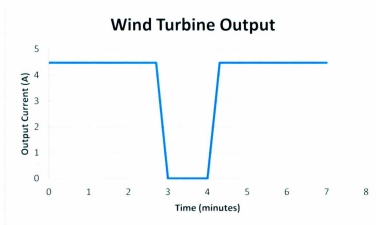


Figure 5.8: Wind current power in first 7 minutes

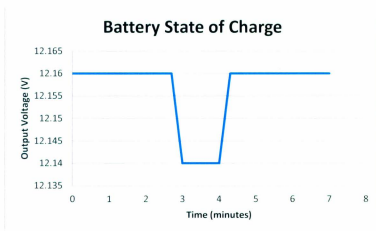


Figure 5.9: Battery state of charge in first 7 minutes





Table 5-2: Experiment results after 30 minutes

Time (minutes)	Battery Voltage (V)	Load Current (A)	PV Current (A)	Wind Current (A)	Diesel generator (PS)
30-33	12.14 v	7.69	2.38	4.47 (4.41-4.60)	off
33-34 decrease the wind speed	12.12 discharging	7.69	0	0	on
34-37	12.14 v	7.69	2.38	4.47 (4.41-4.60)	off

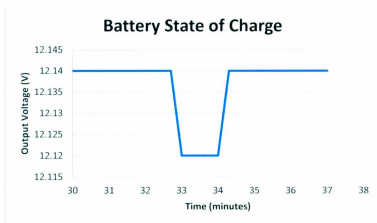


Figure 5.13: Battery state of charge after 30 minutes

### 5.3.1.3 Case study 1 after 50 minutes

Even after 50 minutes of starting the experiment the wind and PV currents are still at the same level. Battery charging level is changed as shown in table 5.3 and figure 5.14.

Table 5-3: Experiment results after 50 minutes

Time (minutes)	Battery Voltage (V)	Load Current (A)	PV Current (A)	Wind Current (A)	Diesel generator
50-53	12.14 v	7.69	2.38	4.47 (4.41-4.60)	off
53-54 decrease the wind speed	12.11 discharging	7.69	0	0	on
54-57	12.14 v	7.69	2.38	4.47 (4.41-4.60)	off

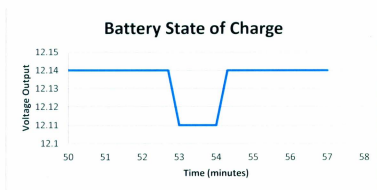


Figure 5.14: Battery state of charge after 50 minutes

### 5.3.2 Case study 2

In the second test, there is no wind (wind speed is zero). The results are shown in table 5.4. The control set the PV for one minute even if the PV cannot handle the load. The PV supply did not meet the load demand, and the battery discharging was very clear in figure 5.15.

**Table 5-4: Experiment results when there is no wind**

Time (minutes)	Battery Voltage (V)	Load Current (A)	PV Current (A)	Wind Current (A)	Diesel generator
70-71	12.11 v	7.65	2.41	0	off
71-72	12.06 discharging	7.65	0	0	on
72-73	12.08 v	7.65	2.41	0	off

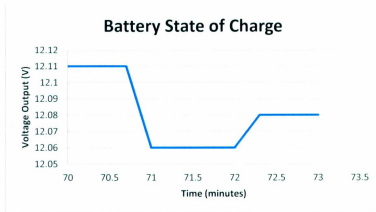
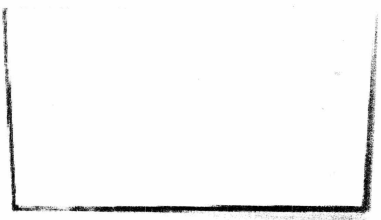


**Figure 5.15: Battery state of charge when there is no wind**



### 5.3.3 Case study 3

The third step was a test on a cloudy day a few days after the first two steps were tested. In the first two steps the power supply was set on 13V, while in the last step it was set on 20V. Table 5.5 shows the results when the wind speed was 10m/s. Figure 5.18 shows the battery state of charge while figure 5.19 and 5.20 show the Wind and PV output current obtained from the scope.

**Table 5-5: experiment results on a cloudy day**

Time (minutes)	Battery Voltage (V)	Load Current (A)	PV Current (A)	Wind Current (A)	Diesel generator
1-2	12.03 V	7.65	0	4.47 (4.41-4.60)	off
2-3	12.09	7.69	0	0	on
3-4	12.03 V	7.72	0	4.47 (4.41-4.60)	off

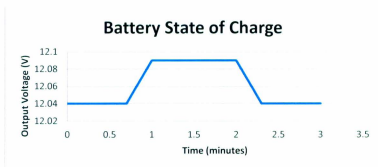


**Figure 5.18: Battery state of charge**

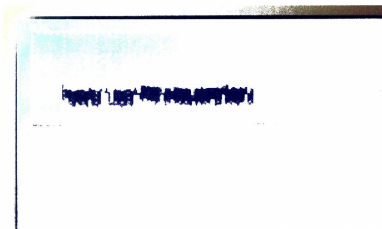


Figure 5.19: Scope display of wind and PV output on a cloudy day 1

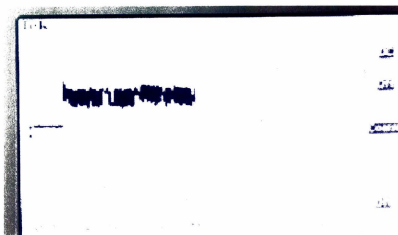


Figure 5.20: Scope display of wind and PV output on a cloudy day 2

#### 5.4 Experiment Results with Battery Connected and Disconnected

Figure 5.21 shows the brightness of the bulb lights when the load is connected to the renewable systems (Wind and PV) and Battery. Figure 5.22 shows less brightness in the



### 5.5 Experiment Results when only Wind Turbine is Connected

When wind speed increased to the maximum which is 14.50m/s in the tunnel (8.7m/s where the wind turbine is) and without battery backup, the light bulbs were less bright. However, the controller was set to control the wind turbine and power supply. Figure 5.23 shows the wind turbine and PV panel output current obtained from the scope while table 5.6 shows the results.

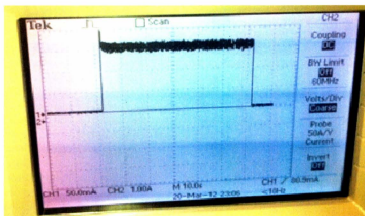


Figure 5.23: Scope display of wind and PV output when only the wind turbine is the connected

Table 5-6: Experiment results when only the wind turbine is the connected

Time (minutes)	Battery Voltage (V)	Load Current (A)	PV Current (A)	Wind Current (A)	Diesel generator
1-4	0	5.94	0	6.15	off
4-5	0	5.94	0	0	on
5-10	0	5.94	0	6.15	off

## **5.6 Summary**

The modeling results of the combined system, which include two wind turbines, photovoltaic subsystem, diesel generator, and battery, are presented in this chapter. Then, many different scenarios of the experiment have been tested and the results are presented as well. Three different cases are tested: sunny day, cloudy day, and zero wind speed.

## Chapter 6 Conclusion and Future Work

### 6.1 Conclusion

Providing uninterrupted power is the main issue for remote areas. Telecommunication towers located in remote locations are generally powered using diesel generators and batteries. However, diesel generators require a higher maintenance cost and for remote sites this cost is very high due to the added oil transportation cost. To provide better network services, BellAliant has started installing hybrid renewable energy systems for its mobile base stations in remote areas. The objective of this research is to design an integrated hybrid power system for a telecommunication facility. This site is located in Mulligan village, Canada, where electric distribution grids have not yet reached. The current system has the continual use of a Perkins 404C-22G diesel generator running at 1800rpm and 2 strings of VRLA GNB XL3000 (3000Ahr per string) batteries.

The proposed system is a combination of renewable and non-renewable power systems. Two BWC-Excel-R/48 with rated capacity of 7.5kW each provide 48V DC, twenty STP280-24/Vd solar modules provide a total of 5.6kW, a Perkins 404C-22G diesel generator is used, with a rated capacity of 20kW, and two strings of VRLA GNB XL3000 batteries are used at Mulligan village. Each battery is 2V and has a capacity 3000Ah with 48V total bus voltage. Wind and PV are the primary power sources of the system and a diesel generator is used as a backup for the long-term storage system, while the battery is used in the system as a backup for the short term storage system.

Before presenting the size, modeling, and experimental results, a brief introduction of the hybrid power system has been presented. Also, some papers related to renewable energy in telecommunication, optimization and modeling of hybrid renewable energy systems, control methods in renewable energy systems, and supervisory control in renewable energy systems have been highlighted.

The results of both the existing and proposed systems are shown in chapter 2. Both systems are simulated in HOMER software, and the optimal results were obtained for each case. The cost difference between the two systems is \$1,045,258 which is a very significant amount for a small system. Diesel generator run times are reduced and the diesel generator in the proposed system will produce only 2% of the total power production. Moreover, the reduction of yearly diesel fuel consumption from 12,672L to 335L has a large impact on the environment and will reduce the helicopter trips to the site. Also, the diesel generator will require less maintenance and have a lower operation cost and a longer service period before replacement.

The details of system components, which include a wind energy conversion system, solar energy conversion system, diesel generator, and battery, have been elucidated. All of these components are modeled in Matlab/Simulink individually. The wind energy systems have been simulated with different wind speeds, and power curves have been validated by comparing them to the manufacturing curves. In addition, the solar energy system has been simulated with different solar irradiance, and power curves have been validated as well. Moreover, the combination system is simulated in Matlab/Simulink

with different scenarios and results have been presented in chapter 5 and proved the sizing (HOMER) results.

The final part of this research is to design a real time supervisory control for the same system scale. Because there are no large system components at Memorial University of Newfoundland, a real time supervisory control was designed and implemented for a small scale system. An Air-X wind turbine with 400W, Coleman solar panels with 120W, power supply, and car battery are used in this system. The microcontroller is programmed by mikroBasic to monitor and control the system. Many different scenarios have been used in the experiment and the results of all those cases have been shown in chapter 5. The results have shown how the supervisory control is expected to perform.

In conclusion, the pre-feasibility study of the Mulligan site shows that using PV and wind are viable solutions for this site. Although the Total Net Present Cost (TNPC) is very high, using a renewable hybrid energy system for this site, but it is much better than using the diesel generator alone. It will reduce overall diesel run times.

## **6.2 Research Contribution**

The contribution of this research can be summarized by the following:

- HOMER software is used to determine the best optimal sizing and a pre-feasibility study of the system and sensitivity analysis is done when designing the system.
- A comparison between the existing and the proposed systems has been made based on system cost and emissions.
- System components have been modeled in Matlab/Simulink individually first and then a combination system has been modeled.

- Different scenarios have been considered for wind and solar subsystems.
- An experimental setup has been done in the Fluid Lab at Memorial University.
- A microcontroller has been programmed by mikroBasic to monitor and control the system.
- A real time on/off supervisory controller has been proposed and implemented for a small scale system.

### **6.3 Future Work**

The system was simulated in Matlab/Simulink for 5 sec which is too short a time to comprehend all the transient characteristics of the system, and the performance of the battery bank has not been included because of the small simulation time limit. Therefore, competitive computer software might be used for a longer duration of the simulation to obtain better results and to include the study performance of the battery bank.

The controlling system is one of the most important parts in designing hybrid power systems. All the system components work individually very well, though some of them do not have a controller system. These controllers do not aim at precise control of the whole system. Therefore, some additional controllers are highly recommended for some power components.

A real time supervisory controller has been implemented for a small scale system. It should be implemented for the same scale system to obtain the desired results and be provided to the BellAliant Company for installing an integrated hybrid power system. The experiment runs for several minutes and the wind speed was controllable. Therefore, the experiment should be run for a few days with uncontrollable wind speed.

The theoretical and experimental work have been carried out for an off grid system. In future work, a connected grid can be considered in both dynamic modeling and for the experimental setup. Also, it can be considered in sizing. Because we have excess power in this system, we will obtain better results if we connect the grid to the system.

**Publications**

1. El Badawe, M.; Iqbal, T.; M, George., "Optimization and a modeling of a stand-alone wind/PV hybrid energy system" presented at *the 25<sup>th</sup> IEEE Conference on Electrical and Computer Engineering, (CCECE 12)*, Montreal, Canada, April 29<sup>th</sup> – May 2, 2012.
2. El Badawe, M.; Iqbal, T.; M, George., "Optimization and a comparison between renewable and non-renewable energy system for a telecommunication site" presented at *the 25<sup>th</sup> IEEE Conference on Electrical and Computer Engineering, (CCECE 12)*, Montreal, Canada, April 29<sup>th</sup> – May 2, 2012.
3. El Badawe, M.; Iqbal, T.; M, George., "Design and dynamic modeling of a hybrid street light system" presented at *IEEE 21, NECEC conference*, St.John's NF, 2011.
4. El Badawe, M.; Iqbal, T.; M, George., "Optimal sizing and modeling of a hybrid energy system for a remote telecommunication facility" presented at *IEEE 21, NECEC conference*, St.John's NF, 2011.

## Bibliography

- [1]. Quaschnig, Volker, "Understanding renewable energy systems", Earthscan, 2005.
- [2]. William H.Kemp, "The renewable energy handbook", Aztext Press, 2009.
- [3]. International Energy Outlook 2011, Energy Information Administration (EIA), <http://www.eia.doe.gov/iea>.
- [4]. Belfkira, R.; Nichita, C.; Barakat, G.; , "Modeling and optimization of wind/PV system for stand-alone site," *18th International Conference on Electrical Machines, 2008. ICEM 2008.*, pp.1-6, Sept 6, 2008.
- [5].Renewables 2011 global statues, Renewable energy policy network for the 21<sup>st</sup> century, <http://www.ren21.net/>.
- [6]. El Badawe, M.; Iqbal, T.; George,M., "Optimization and a modeling of a stand-alone wind/PV hybrid energy system" presented at *the 25th IEEE Conference on Electrical and Computer Engineering, (CCECE 12)*, Montreal, Canada, April 29th – May 2, 2012
- [7]. Bull, S.R.; , "Renewable energy today and tomorrow," *Proceedings of the IEEE* , vol.89, no.8, pp.1216-1226, Aug 2001.
- [8]. J.K. Kaldellis.; , "Optimum hybrid photovoltaic-based solution for remote telecommunication stations," *Renewable energy 2010.*, vol.35, pp.2307-2315 March 23, 2000.
- [9]. Marquet, D.; Foucault, O.; Aubree, M.; , "Sollan-Dimsol R&D Project, Solar and Renewable Energy in France Telecom," *28th Annual International Telecommunications Energy Conference, 2006. INTELEC '06.*, pp.1-8, Sept 10, 2006

- [10]. Lubritto, C.; Petraglia, A.; Vetromile, C.; Caterina, F.; D'Onofrio, A.; Logorelli, M.; Marsico, G.; Curcuruto, S. "Telecommunication power systems: Energy saving, renewable sources and environmental monitoring," *IEEE 30th International Telecommunications Energy Conference, 2008. INTELEC 2008.*, pp.1-4, Sept 14, 2008.
- [11]. Salas, V.; Olfus, E.; Quinones, C.; Vazquez, M.; Rascon, M.; , "Application of hybrid power systems of low power to the remote radio equipment telecommunication," *Proceedings of the 2000 IEEE International Symposium on Industrial Electronics, 2000. ISIE 2000.*, vol.1, pp.174-178, 2000
- [12]. Palm, E.; Heden, F.; Zanna, A.; , "Solar powered mobile telephony," *Second International Symposium on Environmentally Conscious Design and Inverse Manufacturing, 2001. Proceedings EcoDesign 2001.*, pp.219-222, 2001.
- [13]. Smith, S.S.; Iqbal, M.T.; , "Design and Control of a Hybrid Energy System for a Remote Telecommunication Facility ", *presented at IEEE 17. NECEC conference, St.John's NF*, 2007.
- [14]. Nema, P.; Rangnekar, S.; Nema, R.K.; "PV-solar / wind hybrid energy system for GSM/CDMA type mobile telephony base station", *International Journal Of Energy And Environment, 2010*, vol.1, pp.359-366, 2010.
- [15]. Nema, P.; Rangnekar, S.; Nema, R.K.; , "Pre-feasibility study of PV-solar / Wind Hybrid Energy System for GSM type mobile telephony base station in Central India," *The 2nd International Conference on Computer and Automation Engineering (ICCAE), 2010*, vol.5, pp.152-156, Feb 26, 2010.

- [16]. Misak, Stanislav; Prokop, Lukas; , "Off-grid power systems," *9th International Conference on Environment and Electrical Engineering (EEEIC), 2010*, pp.14-17, 16-19 May 2010.
- [17]. Caisheng Wang; Nehrir, H.; , "Power management of a stand-alone wind/photovoltaic/fuel-cell energy system," *IEEE Transactions on Energy Conversion, 2008*, pp.1, 20-24 July 2008.
- [18]. Lagorse, J.; Giurgea, S.; Paire, D.; Cirrincione, M.; Simoes, M.G.; Miraoui, A.; , "Optimal Design Analysis of a Stand-Alone Photovoltaic Hybrid System," *IEEE Industry Applications Society Annual Meeting, 2008. IAS '08*, pp.1-7, 5-9 Oct. 2008.
- [19]. Belfkira, R.; Nichita, C.; Barakat, G.; , "Modeling and optimization of wind/PV system for stand-alone site," *18th International Conference on Electrical Machines, 2008. ICEM 2008*, pp.1-6, 6-9 Sept. 2008.
- [20]. Bajpai, P.; Kumar, S.; Kishore, N.K.; , "Sizing optimization and analysis of a stand-alone WTG system using hybrid energy storage technologies," *2010 Proceedings of the International Conference on Energy and Sustainable Development: Issues and Strategies (ESD)*, pp.1-6, 2-4 June 2010.
- [21]. Razak, N.A.b.A.; bin Othman, M.M.; Musirin, I.; , "Optimal sizing and operational strategy of hybrid renewable energy system using Homer," *2010 4th International Power Engineering and Optimization Conference (PEOCO)*, , pp.495-501, 23-24 June 2010.
- [22]. Reaz Ul Haque; M. T. Iqbal; John E. Quaicoe; , "Sizing, Dynamic Modeling and Power Electronics of a Hybrid Energy System," *Canadian Conference on Electrical and Computer Engineering, 2006. CCECE '06.*, pp.1135-1138, May 2006.

- [23]. Belfkira, R.; Nichita, C.; Reghem, P.; Barakat, G.; , "Modeling and optimal sizing of a hybrid renewable energy system," 13th Power Electronics and Motion Control Conference, 2008. EPE-PEMC 2008., pp.1834-1839, 1-3 Sept. 2008.
- [24]. El Badawe, M.; Iqbal, T.; George, M.; , "Design and dynamic modeling of a hybrid street light system" *presented at IEEE 21. NECEC conference, St. John's NF*, 2011.
- [25]. Tao Chen; Jin Ming Yang; . "Research on energy management for Wind/PV Hybrid power system," *3rd International Conference on Power Electronics Systems and Applications, 2009. PESA 2009.*, pp.1-4, 20-22 May 2009.
- [26]. Becherif, M.; Paire, D.; Miraoui, A.; , "Energy management of solar panel and battery system with passive control," *International Conference on Clean Electrical Power, 2007. ICCEP '07.*, pp.14-19, 21-23 May 2007.
- [27]. Becherif, M.; Ayad, M.Y.; Henni, A.; Wack, M.; Aboubou, A.; , "Hybridization of fuel cell, solar panel and batteries on the DC link for street lighting application," *36th Annual Conference on IEEE Industrial Electronics Society IECON 2010.*, pp.2795-2802, 7-10 Nov. 2010.
- [28]. Ruiz, A.P.; Cirstea, M.; Koczara, W.; Teodorescu, R.; , "A novel integrated renewable energy system modeling approach, allowing fast FPGA controller prototyping," *11th International Conference on Optimization of Electrical and Electronic Equipment, 2008. OPTIM 2008.*, pp.395-400, 22-24 May 2008.
- [29]. Obaid, R.R.; "Grid-tied solar panel and controller for small residential applications", *Int. J. of Thermal & Environmental Engineering*, vol.2, no.2, pp.1.3-106, 2011.

- [30]. Jianping Zhou; Zhiping Wang; Ning Yang; , "Research on inverting control of PV grid-connected LED street lighting system," *2010 International Conference on Information Networking and Automation (ICINA) 2010*, vol.2, pp. 94-96, 18-19 Oct. 2010.
- [31]. Torres-Hernandez, M.E.; Velez-Reyes, M.; , "Hierarchical control of Hybrid Power Systems," *11th IEEE International Power Electronics Congress, 2008. CIEP 2008.*, pp.169-176, 24-27 Aug. 2008.
- [32]. Dai, Renchang; McCalley, James D.; Aliprantis, Dionysios C.; Ajarapu, Venkataramana; Das, Trishna; Wu, Di; Riaz, Muhammad Ali; Imtiaz, Raja Umer; , "Hierarchical control for hybrid wind systems," *North American Power Symposium (NAPS), 2009* , pp.1-6, 4-6 Oct. 2009.
- [33]. Izadian, A.; Heng Yang; Girrens, N.; , "Wind energy harvesting control for green cellphone towers with dSPACE implementation," *37th Annual Conference on IEEE Industrial Electronics Society, IECON 2011*, pp.2511-2516, 7-10 Nov. 2011.
- [34]. Li Wang; Kuo-Hua Liu; , "Implementation of a Web-Based Real-Time Monitoring and Control System for a Hybrid Wind-PV-Battery Renewable Energy System," *International Conference on Intelligent Systems Applications to Power Systems, 2007. ISAP 2007.*, pp.1-6, 5-8 Nov. 2007.
- [35]. Valenciaga, F.; Puleston, P.F.; , "Supervisor control for a stand-alone hybrid generation system using wind and photovoltaic energy," *IEEE Transactions on Energy Conversion*, , vol.20, no.2, pp. 398- 405, June 2005.

- [36]. Dali, M.; Belhadj, J.; Roboam, X.; , "Theoretical and experimental study of control and energy management of a hybrid wind-photovoltaic system," *2011 8th International Multi-Conference on Systems, Signals and Devices (SSD)*, , pp.1-7, 22-25 March 2011.
- [37]. National Renewable Energy Laboratory, <http://www.nrel.gov/>
- [38]. National Aeronautics and Space Administration (NASA).
- [39]. BellAliant Company.
- [40]. Beregy WindPower 2010, "BWC Excel-R/48", available at <http://www.bergey.com>.
- [41]. Saber, A.Y.; Venayagamoorthy, G.K.; , "Plug-in vehicles and renewable energy sources for cost and emission reductions," *IEEE Transactions on Industrial Electronics*, , vol.58, no.4, pp.1229-1238, April 2011.
- [42]. Xiaowen Dong; El-Gorashi, T.; Elmirghani, J.M.H.; , "Renewable energy for low carbon emission IP over WDM networks," *15th International Conference on Optical Network Design and Modeling (ONDM)*, 2011, pp.1-6, 8-10 Feb. 2011.
- [43] Simoes, M. Godoy and Farret, Felix, "Alternative Energy System", CRC Press, Second Edition, 2007.
- [44] Henryson, Mattias and Svensson, Martin, "Renewable Power for the Swedish Antarctic Station Wasa", *Master of Science Thesis, Department of Energy Technology Stockholm, Sweden*, 2004.
- [45] Roberts, Jonas, "Micro Wind Energy Systems in Harsh Environments: Failure Analysis of Small Wind Turbines at Remote Sites in Labrador", *Master of Engineering, Memorial University of Newfoundland*, May 2009.

- [46] Boyle, Godfrey., "Renewable Energy Power for a Sustainable Future", Oxford University Press in association with the Open University, 1996.
- [47] Mohod, S.W.; Aware, M.V.; , "Wind energy conversion system simulator using variable speed induction motor," *2010 Joint International Conference on Power Electronics, Drives and Energy Systems (PEDES) & 2010 Power India*, pp.1-6, 20-23 Dec. 2010.
- [48] Abdal Rassul, Furat.; Abbas.; and Abdulsada, Mohammed., "Simulation of wind-turbine speed control by MATLAB", *International Journal of Computer and Electrical Engineering*, Vol. 2, No. 5, pp.1793-8163, October, 2010.
- [49] Borowy, B.S.; Salameh, Z.M.; , "Dynamic response of a stand-alone wind energy conversion system with battery energy storage to a wind gust," *IEEE Transactions on Energy Conversion*, , vol.12, no.1, pp.73-78, Mar 1997.
- [50] López, Miguel.; Vannier, Jean-Claude., "Stand-alone wind energy conversion system with maximum power transfer control", *Ingeniare. Revista chilena de ingeniería*, vol.17, no.3, pp.329-336, 2009.
- [51] Larry D.Partain, "Solar cells and their application", John Wiley & Sons, Inc, 1995.
- [52] El Badawe, M.; Iqbal, T.; M, George., "Optimal Sizing and Modeling of a Hybrid Energy System for a Remote Telecommunication Facility" *presented at IEEE 21, NECEC conference, St.John's NF*, 2011.
- [53] P Jayarama Reddy, "Science and Technology of photovoltaics", BS Publications, 2010.

- [54] G.N.Tiwari and Swapnil Dubey, "Fundamentals of photovoltaic modules and their applications", RSC Publication, 2010.
- [55] Tariq Iqbal, Renewable energy course lectures, spring 2011.
- [56] Suntech, STP280-24V available at <http://am.suntech-power.com/>
- [57] Chihchiang Hua and Chihming Shen, "Control of DC/DC converters for solar energy system with maximum power tracking", *23rd International Conference on Industrial Electronics, Control and Instrumentation, 1997, IECON 97*. Vol. 2, Nov 1997.
- [58] C.R. Sullivan and M.J. Powers, "A high-efficiency maximum power point tracking for photovoltaic arrays in a solar-power race vehicle", *24th Annual IEEE Power Electronics Specialists Conference 1993, PESC 93*, pp. 574-580, Jun 1993.
- [59] B.K. Bose, P.M. Szczesny and R.L. Steigerwald, "Microcomputer control of a residential photovoltaic power conditioning system", *IEEE Trans. On Industry Applications*, vol. 21, pp. 1182-1191, Sep 1985.
- [60] Mohamed A.S. Masoum, Hooman Dehbonei, and Ewald F.Fuchs, "Theoretical and experimental analyses of photovoltaic system with voltage-and current-based maximum power point tracking", *IEEE Transactions on energy conversion*, vol. 17, December 2002.
- [61] Yves Brunet, "Energy Storage", John Wiley & Sons, Inc, 2011.
- [62] MATLAB/ SimPower System are the products of the MathWorks, available at <http://www.mathworks.com>
- [63] Southwest Wind Power, "Air-X", available at <http://www.windenergy.com>
- [64] Coleman solar panel, available at <http://www.homedepot.com/>

[65] CR5210 current transducer, available at <http://www.crmagnetics.com>

[66] Potter & Brumfield, available at <http://relays.te.com/>

[67] MikroElektronika, available at <http://www.mikroe.com/>

**APPENDICES**

## **Appendix A**

Simulation diagram of the hybrid energy system

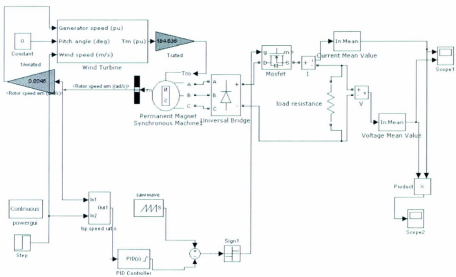


Figure A-1: Simulink model for the wind energy conversion system

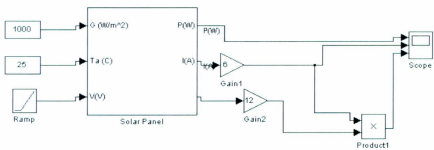


Figure A-2: Simulink model for the solar energy conversion system

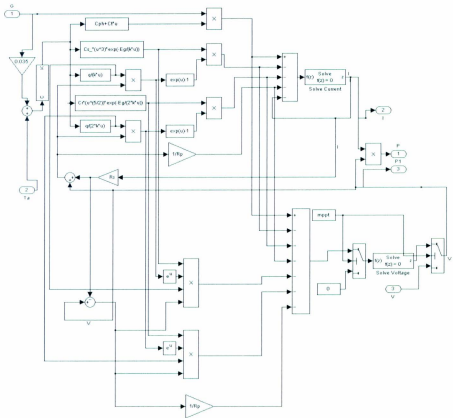


Figure A-3: Subsystem model of the solar cell

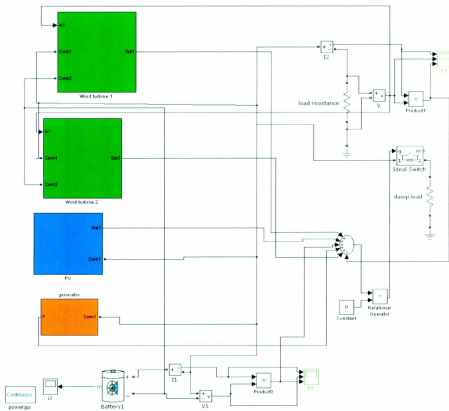


Figure A-5: Simulink model for the whole hybrid power system

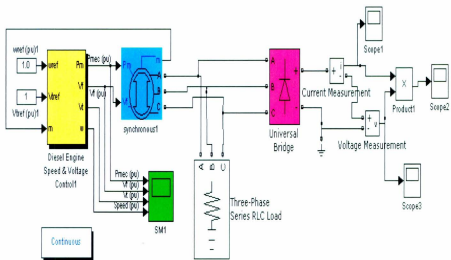


Figure A-4: Simulink model for the diesel generator system

## **Appendix B**

mikroBasic program for the PIC18f4520 microcontroller

mikroBasic program

dim Vw as word

dim Vpv as word

dim VL as word

Main:

ADCON1=\$80

ADCON2=\$87

TRISA=%11111111                   'PORTA is input

TRISB=%00000000                   'PORTB is output

TRISD=%00000000                   'PORTD is output

PORTB=0                           'Wind is off

PORTD=0                           'PV is off

                          'diesel generator is off

Repeat:

setbit(PORTB,1)                   'wind is on

Vw=ADC\_read(0)                   ' exccute conversion and store result in variable Vw

Vpv=ADC\_read(1)                   ' exccute conversion and store result in variable Vpv

VL=ADC\_read(2)                   ' exccute conversion and store result in variable VL

If Vw>VL then

    setbit(PORTB,1)               'wind is on

```

delay_ms(60000)
else
    setbit(PORTB,1)      'wind is on
    delay_ms(100)
    setbit(PORTD,3)      'PV is on
    delay_ms(60000)

end if

if Vw+Vpv>VL then
    setbit(PORTB,1)      'wind is on
    delay_ms(100)
    setbit(PORTD,3)      'PV is on
    delay_ms(60000)
else
    clearbit(PORTB,1)
    clearbit(PORTD,3)
    setbit(PORTD,1)      'diesel generator is on
    delay_ms(60000)
end if
clearbit(PORTD,1)      'Rest Diesel
goto repeat
end.

```







